MONOGRAPH 96-1

The Optical Properties of Sea Ice

Donald K. Perovich

May 1996

Abstract

Sea ice is a translucent material with an intricate structure and complex optical properties. Understanding the reflection, absorption, and transmission of shortwave radiation by sea ice is important to a diverse array of scientific problems, including those in ice thermodynamics and polar climatology. Radiative transfer in sea ice is a combination of absorption and scattering. Differences in the magnitude of sea ice optical properties are due primarily to differences in scattering. Spectral variations are mainly a result of absorption. Changes in such optical properties as the albedo, reflectance, transmittance, and extinction coefficient are directly related to changes in the state and structure of the ice. Physical changes that enhance scattering, such as the formation of air bubbles due to brine drainage, result in larger albedos and extinction coefficients. The albedo is quite sensitive to the surface state. If the ice has a snow cover, albedos are large. In contrast, the presence of liquid water on a bare ice surface causes a decrease in albedo, which is more pronounced at longer wavelengths. Sea-ice optical properties depend on the volume of brine and air and on how the brine and air are distributed.

Cover: Dr. T.C. Grenfell measuring melt pond albedos on first-year ice near Barrow, Alaska. A Kipp radiometer, which measures total shortwave irradiance, is in the foreground. The cylindrical instrument on the tripod is a scanning spectroradiometer that measures spectral irradiance from 400 to 2500 nm.

For conversion of SI units to non-SI units of measurement consult ASTM Standard E380-93, *Standard Practice for Use of the International System of Units,* published by the American Society for Testing and Materials, 1916 Race St., Philadelphia, Pa. 19103.

Monograph 96-1

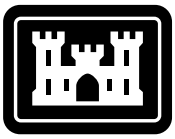

US Army Corps of Engineers
Cold Regions Research & Engineering Laboratory

The Optical Properties of Sea Ice

Donald K. Perovich

May 1996

Prepared for
OFFICE OF NAVAL RESEARCH

PREFACE

This monograph was prepared by Dr. Donald K. Perovich, Geophysicist, Snow and Ice Division, Research and Engineering Directorate, U.S. Army Cold Regions Research and Engineering Laboratory, Hanover, New Hampshire. Funding for this work was provided by the generous support of the Office of Naval Research under Contracts N0001495MP30002 and N0001495MP30031.

The monograph was technically reviewed by J. Richter-Menge and G. Maykut.

The author deeply thanks Dr. T.C. Grenfell for two decades of illuminating, insightful and stimulating discussions on the optical properties of sea ice. The author also appreciates the helpful contributions of G. Cota, A. Gow, B. Light, and G. Maykut. Thanks to K. Jones, R. Maffione, S. Pegau, J. Richter-Menge and W. Tucker for helpful reviews of the manuscript.

CONTENTS

ILLUSTRATIONS

Figure

TABLES

The Optical Properties of Sea Ice

DONALD K. PEROVICH

INTRODUCTION

Sea ice is a translucent material with an intricate structure and complex optical properties. Understanding the reflection, absorption, and transmission of shortwave radiation by sea ice is important to a diverse array of scientific problems. It is of fundamental concern in treating large-scale problems in ice thermodynamics and polar climatology. The summer melt cycle of the Arctic sea ice cover is driven by shortwave radiation, making the interaction of shortwave radiation with sea ice a critical component of the heat balance of the ice cover (Maykut and Untersteiner 1971, Maykut and Perovich 1987, Thorndike 1992, Ebert and Curry 1993). Of particular climatological concern is understanding the sea ice albedo feedback mechanism (Ingram et al. 1989). During the summer the ice cover begins to melt due to the input of solar radiation. This melting tends to decrease the surface albedo and increase the heat input, thereby accelerating the melt process. Because of the climatological interest in the heat balance of sea ice, there is also a need for large-scale spatial and temporal information on ice pack albedos. Properly interpreted, the reflected radiance measured by visible and near-infrared satellite sensors can provide such information. In addition, the amount and spectral composition of shortwave radiation transmitted through sea ice strongly impacts primary productivity and biological activity in and under a sea ice cover (Soo Hoo et al. 1987, Arrigo et al. 1993). Visible light benefits ice biota by contributing to photosynthesis, while ultraviolet light can damage organisms.

This monograph focuses on the optical properties of sea ice. The goal is to provide an introductory tutorial to the topic, not to be a complete compendium of work in the field. The physical principles underlying radiative transfer in sea ice, including scattering and absorption, are discussed, along with the importance to optics of the sea ice physical state and structure. Observational results are presented, with the emphasis placed on explaining the wide variability in sea ice optical properties in terms of ice physical properties and radiative transfer theory. An overview is given of existing sea ice radiative transfer models presenting their basic characteristics, solution schemes, strengths, and limitations. Finally, current research areas and problems of interest in sea ice optical properties are discussed. Since the presence of a snow cover can greatly impact light reflection and transmission through sea ice, some mention is made of the optical properties of snow. An excellent review of the optical properties of snow is provided by Warren (1982). The optical properties of ice biota and particulates found in the ice (Arrigo et al. 1991, Roesler and Iturriaga 1994) are also discussed briefly because of their impact on radiative transfer in sea ice.

BACKGROUND

By "optical" we refer to the portion of the electromagnetic spectrum that is coincident with the wavelength range of radiation from the sun, from roughly 250 nm to 2500 nm (Fig. 1). The solar portion of the electromagnetic spectrum is also referred to as shortwave radiation. The optical region can be divided into three segments: ultraviolet light from 250 to 400 nm, visible light from 400 to 750 nm, and near-infrared light from 750 to 2500 nm. The ultraviolet can be further divided into UV-C from 200 to 280 nm, UV-B from 280 to 320 nm, and UV-A from 320 to 400 nm. Because of strong absorption in the atmosphere, essentially no UV-C reaches the Earth's surface. It is in the UV-B where light levels are substantially enhanced by the depletion of stratospheric ozone (Frederick and Lubin 1988, Lubin et al. 1989, Tsay and

Stamnes 1992, and Smith et al. 1992a) and can have a deleterious impact on living organisms (Smith 1989, Smith et al. 1992b). The familiar spectrum of visible light is also shown in Figure 1 from violet (400 nm) to blue (450 nm) to green (550 nm) to yellow (600 nm) to red (650 nm).

"Properties" refers to the parameters that are used to describe the reflection, absorption and transmission of solar radiation by sea ice. The terminology of radiative transfer is intricate and voluminous. It also has the unfortunate attribute that the same physical quantity may have a different name, depending on whether an oceanographer, an astrophysicist or a biologist is speaking. To avoid a Babel of jargon we shall limit ourselves to the terms needed for a basic understanding of the optical properties and shall follow the terminology conventions of the sea ice literature.

The spectral radiance $I(\theta,\phi,\lambda)$ is the power in a ray of light in a particular direction, where θ is the zenith angle (0 pointing downward, π pointing upward), ϕ is the azimuth angle and λ is the wavelength. The spectral radiance is defined as the radiant flux/nanometer per unit area per unit solid angle in a particular direction and has units of W m^{-2} sr^{-1} nm^{-1}. The spectral irradiance $F(\lambda)$ is simply the radiance projected onto a plane surface and integrated over a hemisphere. Because of this projection the radiance is scaled by $\cos\theta$. The downwelling irradiance $F_d(\lambda)$ is the radiance integrated over downward directions (e.g., from the sky), and the upwelling irradiance $F_u(\lambda)$ is the radiance integrated over upward directions (e.g., from the surface). This can be expressed formally as:

$$F_d(\lambda) = \int_{\phi=0}^{2\pi}\int_{\theta=0}^{\pi/2} I(\theta,\phi,\lambda)\cos\theta\sin\theta\, d\theta d\phi$$

$$F_u(\lambda) = \int_{\phi=0}^{2\pi}\int_{\theta=\pi/2}^{\pi} I(\theta,\phi,\lambda)\cos\theta\sin\theta\, d\theta d\phi \cdot$$

The most studied, and most used, optical property of sea ice is the albedo (α). The spectral albedo is simply defined as the fraction of the incident irradiance that is reflected:

$$\alpha(\lambda) = \frac{F_{u(0,\lambda)}}{F_{d(0,\lambda)}}$$

where the 0 designates the surface. In sea ice thermodynamic studies the wavelength-integrated, or total, albedo α_t is often a quantity of interest, since it is a measure of the total solar energy absorbed by the ice and ocean (Maykut and Untersteiner 1971, Maykut and Perovich 1987). It can be expressed in terms of the spectral albedo and the spectral incident irradiance as

$$\alpha_t = \frac{\int \alpha(\lambda) F_d(0,\lambda)\, d\lambda}{\int F_d(0,\lambda)\, d\lambda} \cdot \qquad (1)$$

The total albedo depends on the spectral distribution of the incident irradiance as well as on the spectral albedo of the surface. Thus a change in cloud conditions, and thereby the incident spectral irradiance, can result in changes in the total albedo (Grenfell and Maykut 1977).

For some problems a knowledge of the angular distribution of the reflected radiance is needed. For example, in climate studies it would be useful to derive large-scale ice albedos from satellite data. However, satellite sensors have narrow fields of view and measure reflected radiance. The key then is to relate the radiance reflected at the viewing angle of the instrument to the albedo of the ice. In order to do this the angular distribution of reflected radiance, characterized by the bidirectional reflectance distribution function (BRDF), must be known. The formal definition of the BRDF is (Nicodemus et al. 1977, Warren 1982, Perovich 1994)

$$R(\theta_0,\theta,\phi_0,\phi,\lambda) = \frac{dI(\theta,\phi,\lambda)}{\cos(\theta_0)\, dF(\theta_0,\phi_0,\lambda)}$$

where θ_0 and ϕ_0 are the solar zenith and azimuth angle, $F(\theta_0, \phi_0, \lambda)$ is the incident spectral irradiance, and R has units of steradians^{-1}. Formally R is a derivative quantity, similar to a probability density function, defined in terms of infinitesimal angles. In practice, the definition is extended to finite, measurable angles, so that $dI \rightarrow \Delta I$ and $dF \rightarrow \Delta F$.

Light transmission through the ice is characterized by the transmittance $T(\lambda)$, which is similar to the albedo in that it is the fraction of the incident irradiance that is transmitted through the ice. Light attenuation in the ice is often represented using an irradiance extinction coefficient

$$\kappa(z,\lambda) = \frac{-1}{F_d(z,\lambda)} \frac{dF_d(z,\lambda)}{dz}$$

where $F_d(z, \lambda)$ is the downwelling spectral irradiance at depth z in the ice.

Let us now examine the difficulties in deter-

mining the optical properties of sea ice by posing a simply stated question: "What is the albedo of sea ice?" Albedos are straightforward to determine. A radiometer is used to measure the irradiance incident on a surface and reflected from the surface. The albedo is constrained to lie between 0, if none of the incident irradiance is reflected, and 1, if all the incident is reflected. At first glance this appears to be an easy question to answer.

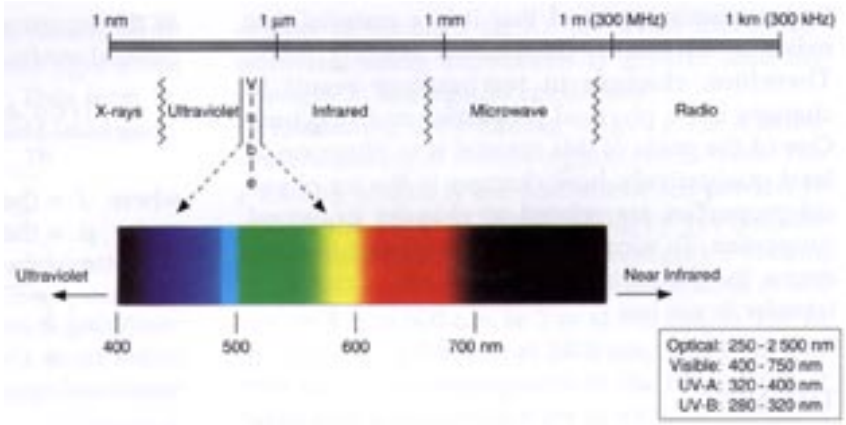

Figure 1. The optical portion of the electromagnetic spectrum. Visible light is from 400 nm (violet) to 750 nm (red).

Figure 2 is an aerial photograph of a small, roughly one-quarter-square-kilometer, area of a typical summer Arctic scene. The melt season has begun and there is a tremendous amount of spatial variability in ice surface conditions: snow-covered ice, bare white ice, blue melt ponds, dirty ice, and areas of open water. This variability is also manifested in the wavelength-integrated albedo, which ranges from 0.05 for open water, to 0.2 to 0.4 for ponded ice, to 0.5 to 0.7 for bare ice, to 0.75 to 0.85 for snow-covered ice. Observations of wavelength-integrated albedo for a full range of sea ice types and conditions are summarized in Figure 3. Considerable variability in albedo is apparent. Determining that the albedo falls between 0.05 and 0.9 still does not provide an adequate answer to our question of "What is the albedo of sea ice?" Indeed, while the question is simple to state, it is extremely difficult to answer on a large scale.

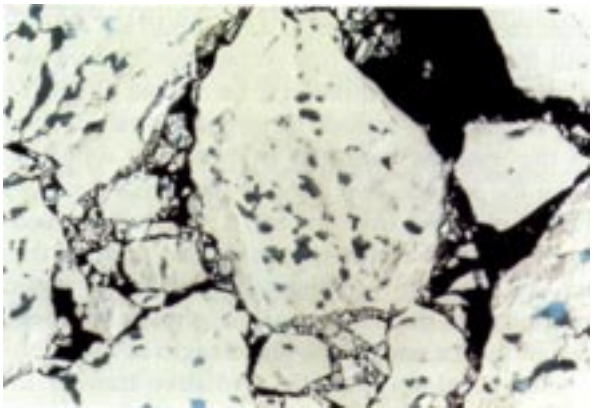

Figure 2. Aerial photograph of typical Arctic summer scene taken from an altitude of 600 m on 3 August 1994 at 78°N, 177°W. The horizontal extent is approximately 425 m.

Considering the complicated and variable physical structure of sea ice, variability in the optical properties should not be surprising. To understand and explain this variability, it is necessary to examine the physical state and structure of the ice. As Figure 2 indicates, sea ice exhibits a great degree of horizontal variability with diverse surface conditions, including ponds, bare ice, and snow-covered ice, and thicknesses that range from open water to pressure ridges over 10 m thick. There is also vertical complexity, with ice properties such as temperature, salinity, brine volume and air volume changing significantly from the ice surface to the ice/water interface. The details of sea ice physical properties and structure are summarized in Weeks and Ackley (1982). What is most germane to optics is that sea ice has an intricate structure consisting of an ice matrix with inclusions of air, brine, solid salts

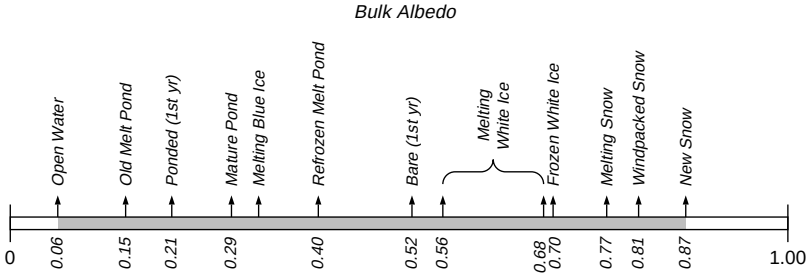

Figure 3. Range of observed values of total albedo for sea ice. The albedos are from Burt (1954), Chernigovskiy (1963), Langleben (1971), Grenfell and Maykut (1977), and Grenfell and Perovich (1984).

and contaminants, and that it is a material that exists at its salinity-determined melting point. Therefore, changes in temperature result in changes in its physical properties and structure. One of the goals of this tutorial is to illustrate, at least qualitatively, how changes in the ice physical properties are related to changes in optical properties. To accomplish this, we must first examine the theoretical underpinnings of radiative transfer in sea ice.

THEORY

The interaction of solar radiation with sea ice is illustrated schematically in Figure 4. The incident radiation field consists of a direct beam component from the sun and a diffuse component from the sky and clouds. If it is completely cloudy and the solar disk is not visible, the incident radiation field is considered to be diffuse. Depending on sky and surface conditions some portion of the incident radiation is specularly reflected from the surface. A portion of the incident radiation is reflected from the ice, a portion absorbed in the ice, and a portion transmitted through the ice. As we shall see, the relative sizes of these portions are dependent on the physical properties of the ice and on the wavelength of the light.

At optical wavelengths, radiative transfer in sea ice is governed by two processes: absorption and scattering. As a ray of light passes through sea ice, some of the light is absorbed by the ice and some of it is scattered from the beam in different directions. This is expressed more formally

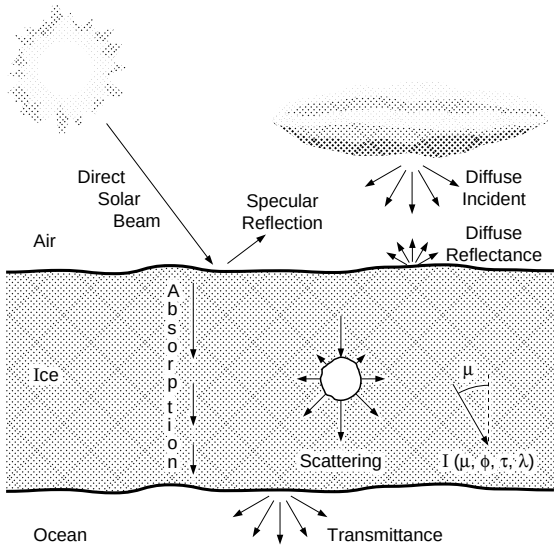

Figure 4. Schematic of radiative transfer in sea ice.

as the equation of radiative transfer for a plane parallel medium (Chandrasekhar 1960):

$$-\mu \frac{dI(\tau,\mu,\phi,\lambda)}{d\tau} = I(\tau,\mu,\phi,\lambda) - S(\tau,\mu,\phi,\lambda) \quad (2)$$

where I = the radiance
μ = the cosine of the zenith angle θ
ϕ = the azimuth angle.

Scattering is included in the S term, which is referred to as the source function. τ is the nondimensional optical depth and is defined as

$$\tau(\lambda) = \left[k(\lambda) + \sigma(\lambda)\right] z$$

where k is the absorption coefficient, σ is the scattering coefficient, and z is the physical depth. The single scattering albedo

$$\varpi_0(\lambda) = \frac{\sigma(\lambda)}{k(\lambda) + \sigma(\lambda)}$$

gives the fractional loss due to scattering (Chandrasekhar 1960, Mobley 1994). ϖ_0 ranges from 0 for a purely absorbing medium to 1 for a purely scattering medium. A plane parallel medium is horizontally homogeneous, but can have vertical variations.

The compact form of eq 2 belies its true complexity. This complexity becomes evident if there is scattering in the medium ($\varpi_0 > 0$) and the source function is expressed in detail. For a plane-parallel medium with a direct incident beam, the source function is expressed as

$$S(\tau,\mu,\phi,\lambda) = \frac{\varpi_0}{4\pi} \int_{-1}^{1} \int_{0}^{2\pi} p(\mu,\mu',\phi,\phi') I(\tau,\mu,\phi,\lambda)$$

$$d\mu' d\phi - \frac{E_0(\lambda)}{4} p(\mu,\mu',\phi,\phi') e^{-\tau(\lambda)/\mu_0},$$

where $p(\mu,\mu',\phi,\phi')$ is the phase function and E_0 is the radiance of the direct beam component of the incident radiation field. With scattering included, eq 2 is an integro-differential equation and is not readily amenable to solution. However, while it is difficult to solve the equation, it is still straightforward to understand qualitatively. The double integral term is used for diffuse radiative processes only and represents scattering of the radiance field $I(\tau,\mu',\phi',\lambda)$ from different directions into the direction of the solution (μ,θ). How much of this light is scattered from one direction to another is defined by the phase function $p(\mu,\mu',\phi,\phi')$. The phase function is normalized so that its in-

tegral over angle is equal to one. The second term provides the contribution of scattered light from the attenuated direct beam $E_0(\lambda)$. This term is needed only if there is direct incident irradiance as well as a diffuse component.

Absorption

It is time to examine absorption and scattering in sea ice in detail, starting with absorption because it is the simpler of the two processes. Consider the case of absorption only for a direct beam of light normally incident on a medium. Since there is no scattering, $S = 0$ and $\sigma = 0$. For normal incidence, $\theta = 0$, which means $\mu = 1$. Equation 2 then reduces to

$$\frac{-dI(z,\lambda)}{k(\lambda)dz} = I(z,\lambda)$$

which, when solved, gives the familiar exponential decay law

$$I(z,\lambda) = I(0,\lambda)e^{-kz} \tag{3}$$

also known as Beer's law or the Bouguer-Lambert law. Radiative transfer in a purely absorbing medium is quite simple to describe. The radiance decreases exponentially with depth in the medium, with the rate of decrease dependent on the absorption coefficient. What needs to be known are the absorption coefficients for the primary components of sea ice: ice, brine and air. Equation 3 implies that absorption coefficients can be determined by measuring the incident radiance, the transmitted radiance, and the thickness of a homogeneous sample that is free of scatterers (Grenfell and Perovich 1981).

Absorption in the air inclusions in sea ice is negligible, so absorption coefficients for air are assumed to be zero. Spectral absorption coefficients from the ultraviolet to the near-infrared for ice and seawater are shown in Figure 5. Absorption coefficients for ice were determined using pure, bubble-free, fresh ice (Grenfell and Perovich 1984, Perovich and Govoni 1991), and absorption coefficients for brine taken from measurements of clear Arctic water (Tyler and Smith 1970, Smith and Baker 1981). The minimum absorption and therefore maximum transmission for ice is in the blue part of the electromagnetic spectrum at 470 nm. Spectral changes in absorption coefficient are extremely large, spanning several orders of magnitude from 250 to 1400 nm. Spectral differences in the transmitted radiance, $I(z, \lambda)$, are even more pronounced, being exponentially greater than the changes in absorption coefficient.

Examining the *e*-folding length gives a better understanding of the absorption coefficients. The *e*-folding length is the amount of ice needed to reduce the incident light ($I(0, \lambda)$) by $1/e$ (i.e., the transmitted light is 37% of the incident). *e*-folding lengths for ice decrease sharply from 24 m at 470 nm, to 8 m at 600 nm, to 2 m at 700 nm, to 0.05 m at 1000 nm, to 0.006 m at 1400 nm. This indicates that ice is quite transparent in the blue, while it takes only a few centimeters of ice to absorb most of the light beyond 1000 nm.

As Figure 5 indicates, absorption coefficients for clean Arctic water are similar in magnitude and spectral shape to values for pure ice. An absorption coefficient for sea ice k_{si} is determined by combining the absorption coefficients for the constituent components of brine and ice using

$$k_{si} = \nu_i k_i + \nu_b k_b \tag{4}$$

where ν_i and ν_b represent the volume fraction of ice and brine, and k_i and k_b are the absorption

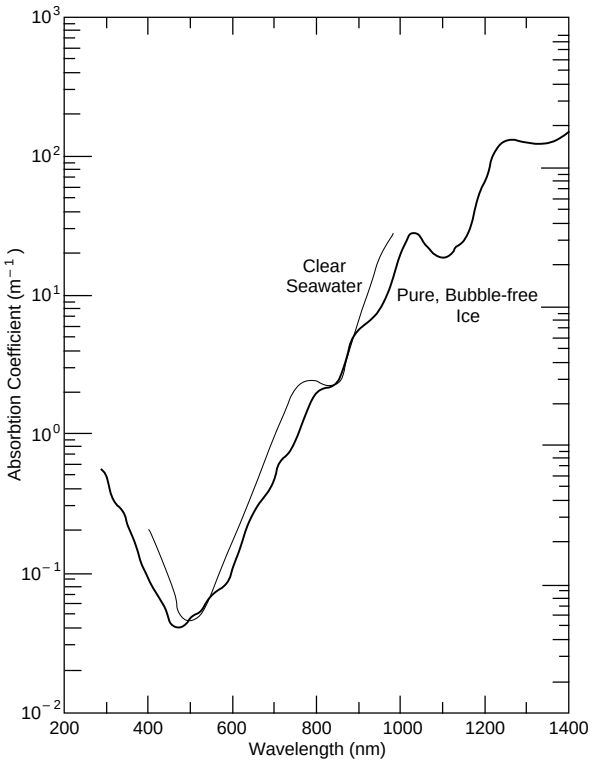

Figure 5. Absorption coefficients of pure, bubble-free ice (Grenfell and Perovich 1981, Perovich and Govoni 1991) and clear sea water (Tyler and Smith 1970, Smith and Baker 1981).

coefficients of ice and brine (Grenfell 1983). Absorption by air is assumed to be negligible.

Equation 4 provides a simple means of generating an absorption coefficient for sea ice from physically determinable quantities and known values of ice and brine absorption coefficients. Unfortunately, in nature, sea ice is often more than a combination of ice, brine and air. For example, particulates, sediments, ice biota and dissolved organics can be present. If these impurities are present in sufficient quantity, then their absorptive properties must also be considered. In general these impurities are strongly absorbing and weakly scattering. Absorption coefficients for sediments and ice biota vary depending on their composition. Examples of absorption coefficients for ice biota (Arrigo et al. 1991) are shown in Figure 6. The spectral shapes of these absorption coefficients are quite different than those of ice or brine. If sediment or ice biota are present in sufficient quantity, they should be explicitly treated in the theoretical formulation by modifying eq 4.

Scattering

Sea ice is not a monolithic slab of pure ice. It has an intricate structure consisting of an ice matrix with inclusions of brine, air and perhaps solid salts. Since these inclusions have different indices of refraction than the surrounding ice, they scatter light. The larger the difference in index of refraction between the inclusion and the ice, the stronger the scattering. Sea ice has an abundance of brine pockets and air bubbles and therefore is a highly scattering medium. In certain cases, particulates, sediment, and ice biota contribute to scattering, but air bubbles and brine pockets are the primary scatterers in sea ice and are the focus of this discussion.

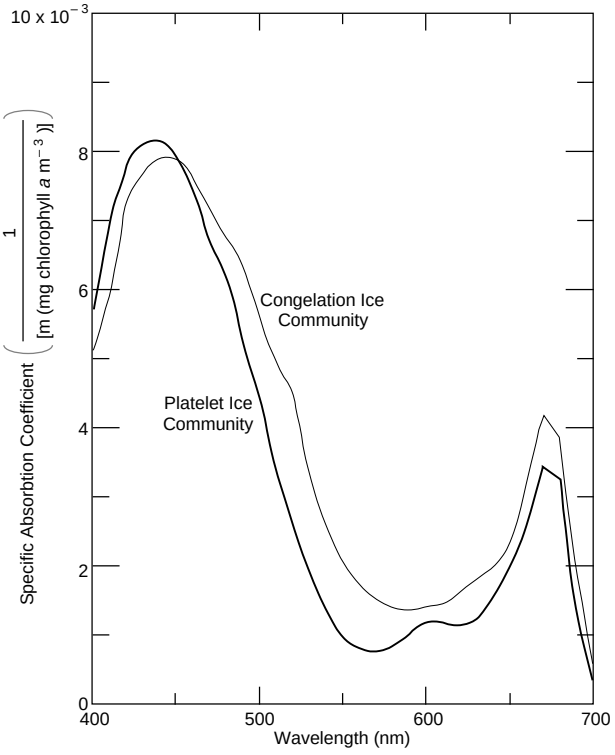

Figure 6. Absorption coefficients of biota found in congelation ice and frazil ice (from Arrigo et al. 1991).

Scattering results from differences in the real indices of refraction (n) between ice ($n \sim 1.31$) and the inclusions. With a greater difference in index of refraction, air bubbles ($n \sim 1.0$) are more strongly scattering than brine pockets. The real part of the index of refraction for brine depends on temperature, increasing from 1.34 at –2°C to 1.40 at –32°C (Maykut and Light 1995). If the ice is cold enough that solid salts form, scattering increases significantly, since these salts are very effective scatterers (Perovich and Grenfell 1981). The scattering coefficient depends not only on the amount of brine and air, but on how it is distributed. This complicates matters since the readily determined brine and air volumes are not sufficient to define scattering. The more difficult to obtain size distribution of the inclusions is also needed. More inclusions in the ice results in more scattering and consequently a larger scattering coefficient. Scattering coefficients in sea ice are large, with values typically greater than 10 m^{-1} for warm ice and greater than 200 m^{-1} for ice with abundant air bubbles or ice colder than –24°C with precipitated hydrohalite present (Perovich and Grenfell 1982).

Scattering is defined by two parameters: the scattering coefficient and the phase function. The scattering coefficient (σ) is analogous to the absorption coefficient and is a measure of the amount of scattering per unit length. The phase function [$p(\mu,\mu',\phi,\phi')$] describes the angular dependence of scattering and usually is normalized so that its integral over the full range of μ and ϕ is equal to one.

Because scattering depends on the intricate and highly variable microstructure of sea ice, it is not possible to formulate a simple, all-encompassing equation to define the scattering coefficient and the phase function, as we could for the absorption coefficient. Complicating matters even further is the fact that in a highly scattering medium such as sea ice, scattering coefficients and phase

functions are extremely difficult to measure. There is, however, one simplifying aspect to scattering in sea ice in the optical regime: it can be assumed to be independent of wavelength. The wavelength dependence of the real portion of the index of refraction for ice, brine and air is very weak at optical wavelengths and typically is assumed to be constant with wavelength (Grenfell 1983, 1991). Optical wavelengths are on the order of tenths of a micrometer to micrometers. The inclusions in sea ice have sizes on the order of tenths of a millimeter for brine pockets to millimeters for air bubbles. Since the scatterers are much bigger than the wavelength and the scatterers are far apart, contributions due to diffraction and interference can be ignored (Grenfell 1983, Bohren and Huffman 1983). The result of the weak wavelength dependence of n, and the fact that the size of the scatterers is much larger than the wavelength, is that scattering coefficients and phase functions for sea ice can be assumed to be constant with wavelength (Grenfell 1983, 1991, Perovich 1993). A similar argument is made when analyzing scattering in snow (Bohren and Barkstrom 1974, Wiscombe and Warren 1980). A thorough general discussion of scattering can be found in van de Hulst (1981) and Bohren and Huffman (1983).

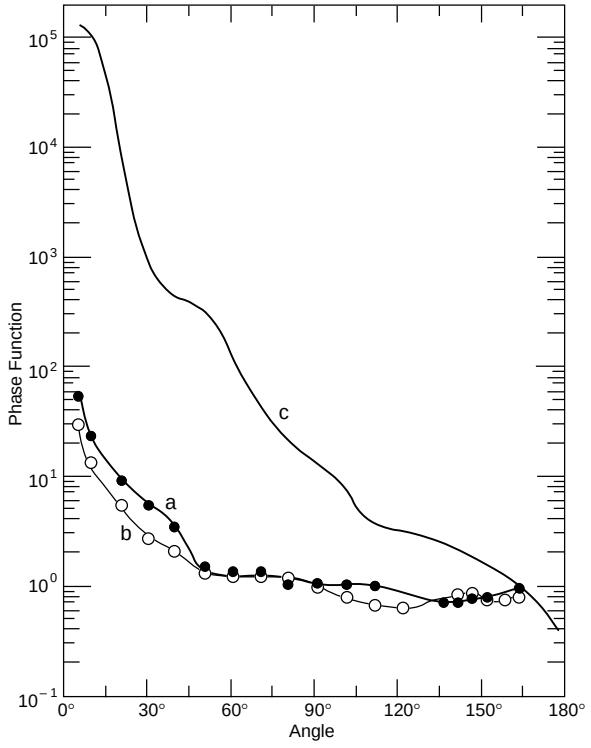

Figure 7. Observed (Grenfell and Hedrick 1983) and calculated (from Light 1995) phase functions for sea ice. 0° is forward scattering and 180° is backward scattering: a) observations of ice grown at –30°C, b) observations of ice grown at –10°C, and c) calculated estimates for ice at –30°C.

Observations of scattering parameters are limited. Perovich and Grenfell (1982) estimated scattering coefficients for young ice from observations of albedo and transmittance. They found that scattering coefficients ranged from 8.9 m^{-1} for melting young ice to 19.6 m^{-1} for cold young ice to 420 m^{-1} for very cold young ice with precipitated solid salts present. Grenfell and Hedrick (1983) used small samples of young ice to measure phase functions for sea ice. Phase functions for columnar ice samples grown at –10°C and –30°C are shown in Figure 7. The phase function is strongly forward-peaked, with forward scattering being more than a factor of 50 greater than side or backward scattering. However, although small samples were used, there was still multiple scattering, and consequently the results represent only an approximation to the true single scattering albedo and phase function. Multiple scattering tends to smooth and reduce the angular dependence of the measured phase function.

Numerical calculations have been used to supplement the relatively sparse observational data (Grenfell 1983, 1991). Phase functions are calculated using a Mie scattering model with the indices of refraction for ice and brine and inclusion size distributions as input parameters (Bohren and Huffman 1983). A calculated phase function for sea ice at –30°C with brine pockets with a radius of 0.02 mm (Light 1995) is compared to observed values in Figure 7. As expected, the calculated phase function is more strongly forward-peaked than the multiply-scattered observed.

Though we do not have a quantitative understanding of the relationship between scattering and ice physical properties, a qualitative grasp is sufficient for our purposes. To interpret observations of optical properties the important theoretical points are 1) absorption coefficients for ice and brine depend strongly on wavelength, 2) scattering coefficients and phase functions for sea ice are constant with wavelength, 3) increasing the number of inclusions in sea ice increases the amount of scattering, 4) air bubbles scatter more strongly than brine pockets, and 5) scattering in sea ice is strongly forward peaked. With this theoretical foundation regarding the underlying physics of radiative transfer in sea ice, it is time to revisit the question of "What is the albedo of sea ice?"

OBSERVATIONS

There is a large observational dataset of sea ice optical properties, particularly of sea ice albedos (Perovich et al. 1986). In this section we present an overview of these observations in the context of illustrating how the optical properties of sea ice are affected by the physical properties. We investigate the effects of ice type, surface conditions, ice thickness, ice brine volume, and impurities on albedo, reflectance, transmittance, and extinction coefficient. The simplifying beauty of optical property observations is that, at least from 400 nm to 750 nm, what you see is what you get. If the ice looks white, then its albedo will be high and relatively constant with wavelength. Similarly, the spectral albedo of a blue-looking melt pond will have a peak between 400 and 500 nm.

Albedos

Albedos are sensitive to thickness during the initial stages of ice growth. Weller (1972) measured total albedos in a freezing lead and found a rapid rise in albedo from 0.08 to 0.40 as the ice grew from open water to a thickness of 0.30 m, followed by a more gradual, asymptotic increase as the ice continued to grow. For ice thicker than approximately 0.8 m total, albedo shows little change with thickness (Maykut 1982).

Spectral changes in albedo during initial ice growth are plotted in Figure 8. The ice was grown in the laboratory at a constant air temperature of –20°C and had a columnar crystal structure (Perovich 1979). Albedo increased with thickness at all wavelengths. As the ice grows thicker, opportunities for backscattering in the ice are added and at first albedos rise rapidly. However, the path length of the backscattered light also increases, until finally only a negligible amount of light penetrates to the bottom of the ice, is backscattered, and emerges from the ice surface without being absorbed. At this point increasing the ice thickness no longer directly affects the albedo and the ice is optically thick. As Figure 8 indicates, this asymptotic ice thickness is smaller at longer wavelengths. At shorter wavelengths albedos are still increasing when the ice is 0.25 m thick, while at longer wavelengths (beyond 700 nm), the asymptotic nature of the albedo increase is evident. This is a direct result of the increase in absorption as wavelength increases. This is consistent with our earlier comment: spectral variations in optical properties are due to absorption. A closer look at Figure 8 shows that the rapid rise in albedo did not begin until the ice was 0.05 m thick. During the first 0.05 m of growth, the ice in this experiment had not yet begun to cool and brine volumes were quite large. Because of this there was little scattering in the ice. As the ice cooled and the large brine pockets fragmented into many smaller pockets, there was more scattering and the albedo increased. This observation illustrates again that the optical properties of sea ice are often more complicated than we would expect.

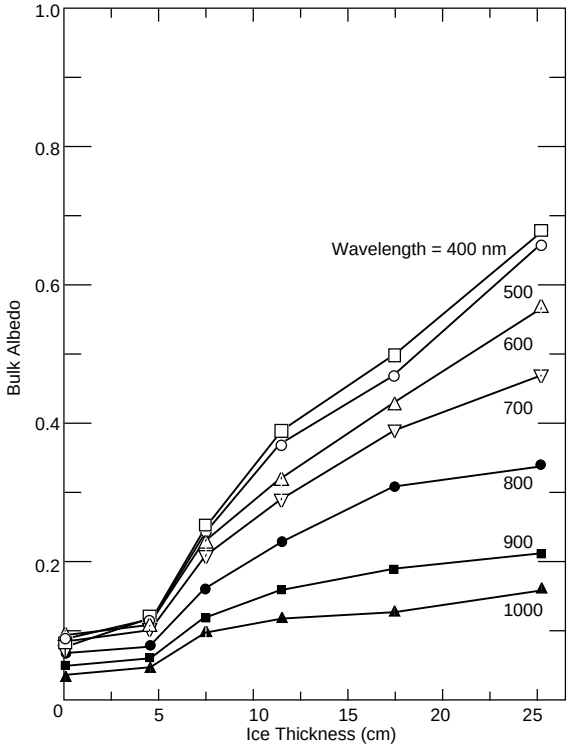

Figure 8. Laboratory observations of the increase in spectral albedo during initial ice growth (Perovich 1979). The ice was grown at an air temperature of –20°C.

Of course, even for thick ice, sea ice albedos vary. From the previous discussion we can see that albedo is sensitive to the ice surface conditions. Spectral albedos for multiyear ice are plotted in Figure 9 (taken from Grenfell and Maykut 1977). These albedos represent a possible evolutionary sequence from spring to summer as melt occurs, and the ice cover changes from snow-covered ice to bare ice or frozen ponds to melting ice to ponded ice. Snow albedos (curve a) are large (~0.9) and nearly constant with wavelength in the visible; the snow appears bright and white. Scattering coefficients for snow are so large that, in the visible, absorption has little impact on the albedo and there is no wavelength dependence.

A 0.1-m-thick layer of wind-packed Arctic snow is sufficient to eliminate any contribution to the albedo from the underlying ice.

Spectral albedos decrease as the surface changes from snow-covered ice to cold, bare multiyear ice (curve b). White multiyear ice typically has a drained bubbly surface layer with plenty of air bubbles which, while not as strongly scattering as snow, still contributes considerable scattering. The result is an overall decrease in albedo of approximately 10% and a slight wavelength dependence. As the ice warms and begins to melt (curve c), albedos continue to decrease with a more evident wavelength dependence. This is due to a decrease in scattering as the ice melts and some of the air voids fill with water. In some areas of the ice cover, water collects on the surface, forming melt ponds (curve d). As the melt season progresses these ponds can get deeper (curve e). Albedos of ponded ice are characterized by a maximum in the 400–500 nm region and a precipitous decrease between 500 and 800. The melt ponds look blue. This spectral behavior is due to the transparency of the water at shorter wavelengths; albedos below 500 nm are determined primarily by the scattering properties of the underlying ice. From 500 to 800 nm the albedo becomes increasingly insensitive to the underlying ice as the absorption in the water becomes the dominant factor. Above 800 nm absorption in the water is so great that pond albedos are essentially determined by Fresnel reflection at the surface and are independent of wavelength. These results indicate that both the magnitude and the shape of the spectral albedos are extremely sensitive to the amount of liquid water present in the upper part of the ice.

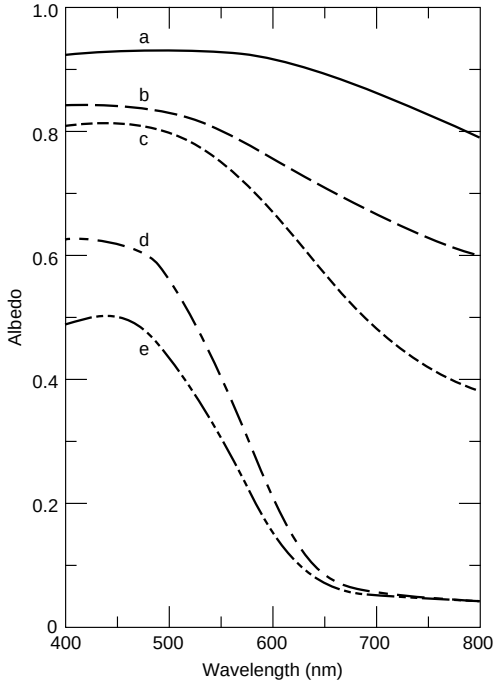

Figure 9. Spectral albedos for a possible evolutionary sequence of multiyear ice (Grenfell and Maykut 1977): a) snow-covered ice, b) cold bare ice, c) melting bare ice, d) early-season melt pond and e) mature melt pond.

When skies are clear, the wavelength interval from 1000 to 2500 nm can contain up to 25% of the total incident shortwave energy (Grenfell and Perovich 1984), so albedos in this region can have a significant impact on the heat and mass balance of the ice. Figure 10 shows a spectral albedo sequence that first-year ice might follow as it progresses through a melt cycle from (a) ice covered by cold dry snow, (b) to ice covered by melting snow, (c) to bare ice with a crumbly surface layer, and (d) to melting first-year blue ice. Concentrating on wavelengths beyond 1000 nm, a continual downward trend is evident, with albedo reaching a minimum at about 1500 nm. Local maxima are located at 1350, 1900 and 2300 nm and correspond to minima in the absorption spectrum for ice. In general, sea ice and snow albedos at longer wavelengths are significantly smaller than values at visible wavelengths.

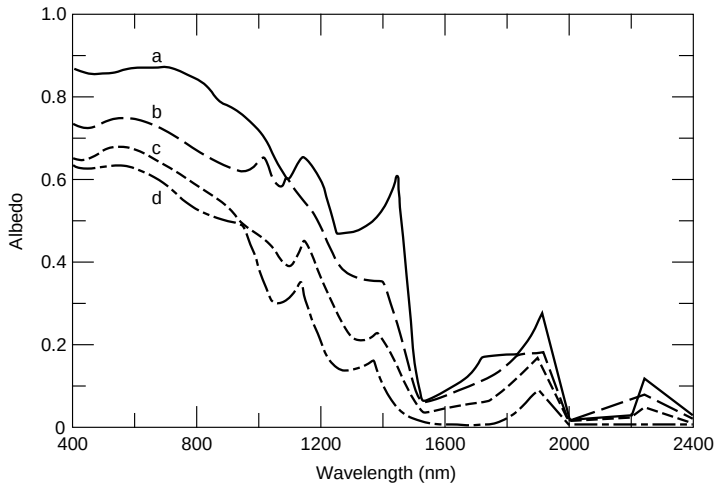

Figure 10. A spectral albedo sequence that first-year ice might follow through a melt cycle (Grenfell and Perovich 1984): a) ice covered by cold dry snow, to b) ice covered by melting snow, to c) bare ice with a crumbly surface layer, to (d) melting first-year blue ice.

Comparing albedos in Figures 9 and 10 demonstrates that, for equivalent conditions, multiyear ice albedos are typically larger than first-year ice values. Multiyear ice has undergone a summer melt season, with the attendant surface melting and brine drainage. This results in a well-developed surface-scattering layer with many air bubbles.

As a result of the decrease in albedo at longer wavelengths, total albedos (α_t) are greater under cloudy skies than under clear skies. The total albedo depends on the spectral albedo and the spectral incident irradiance (eq 1). Clouds absorb more strongly in the infrared than in the visible. Therefore on cloudy days a greater portion of the incident irradiance is at visible wavelengths, where the albedo is larger. Total albedos under cloudy skies are typically 8–12% larger than clear sky values (Grenfell and Maykut 1977, Grenfell and Perovich 1984). When the incident direct beam component is significant, both spectral and total albedos increase as the solar zenith angle increases (sun closer to the horizon) due to enhanced specular reflection (Perovich and Grenfell 1982) and to forward scattering allowing the photons to escape the medium faster.

Surface conditions have a strong impact on albedo, but the internal state and structure of the ice are also significant. As we have seen, the presence of air bubbles in the upper portion of the ice enhances albedo. Brine volume is another important ice physical property that we might expect to have some impact on albedo. Perovich and Grenfell (1981) investigated the influence of brine volume on albedo for young ice. Results from three laboratory experiments are summarized in Figure 11. In each experiment the ice was grown at a selected air temperature (–37°, –30° and –10°C), and therefore a different growth rate, to a thickness of approximately 0.25 m. Brine volume was then varied by warming the ice. For each experiment there is a continual decrease in albedo as brine volume increases. As the ice warmed and the brine volume increased, individual brine pockets coalesced, forming larger but fewer inclusions. Thus, the result of the warming was a reduction in the number of brine pockets and in the amount of scattering. Comparing between experiments, we also see that at a given brine volume there is considerable variability in the observed albedo, with faster grown ice (lower air temperature) having larger albedos (Perovich and Grenfell 1981). More rapidly grown ice has smaller platelet and crystal sizes and more brine inclusions (Weeks and Hamilton 1962, Lofgren and Weeks 1969, Weeks and Ackley 1982). This leads to the important conclusion that not only is the volume of brine important, but how it is distributed is also significant. For a given volume of brine, there is more scattering if that brine is distributed into many small brine inclusions, rather than a single large one. The same conclusion is true for air bubbles.

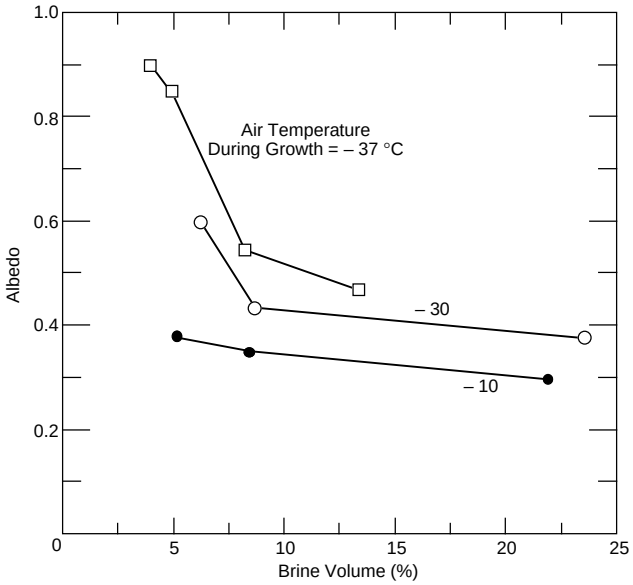

Figure 11. Observations of total albedo vs. brine volume for young ice (from Perovich and Grenfell 1981). Three experiments were performed where the ice was grown to approximately 0.25 m thick and then warmed, in stages, to –2 °C.

All of the albedos presented so far have been for Arctic sea ice. Are albedos for Antarctic ice different? Spectral albedos for young sea ice grown off of East Antarctica are plotted in Figure 12 (Allison et al. 1993). These albedos show the same general properties as Arctic sea ice results; an increase as the ice grows thicker and a gradual wavelength dependence with larger albedos at shorter wavelengths (Schlosser 1988, Allison et al. 1993). There are differences in ice structure between Antarctic and Arctic sea ice. Antarctic sea ice has much more frazil ice than Arctic sea ice and is somewhat more saline (Gow and Tucker 1990). Surface conditions also differ with significant amounts of flooded snow-covered ice but very little ponded ice in the Antarctic (Andreas and Ackley 1982). Because of this there may be differences in optical properties between Antarctic and Arctic sea ice, but any differences *between*

the two cases are smaller than differences *within* the two.

Reflectance

When considering light reflected from sea ice, the albedo is the parameter of prime climatological importance. However, optical remote sensing instruments mounted on aircraft or satellites typically have narrow fields of view and measure reflected radiance, rather than irradiance. To convert these observations of radiance to an estimate of irradiance, information on the bidirectional reflectance distribution function (BRDF) is needed. Under cloudy conditions the incident radiation field is diffuse, so the light reflected from the surface is also diffuse. Reflected radiance is essentially the same in any direction and the reflected irradiance is easily computed. When it is sunny, though, the incident radiation consists of a diffuse sky component plus a very strong solar direct beam, and the incident radiance field is strongly anisotropic. For these incident conditions the angular distribution of reflected radiance can be complex. Angular reflectances (reflected radiance normalized to a white reference standard) measured under sunny skies for snow-covered ice and bare blue ice are plotted in Figure 13. Snow-covered ice reflectances are fairly constant with angle, except for a 30% increase at the angle of reflection of the solar beam. The peak in reflectance at the angle of reflection is even more pronounced in the bare blue ice case, with an increase to nearly twice the value of the albedo. At other angles, blue ice reflectances are equal to or slightly less than the albedo. The differences between R and α show the importance of the BRDF in determining albedos from observations of reflected radiance. The presence of any systematic topographic features, such as sastrugi, will further complicate the BRDF.

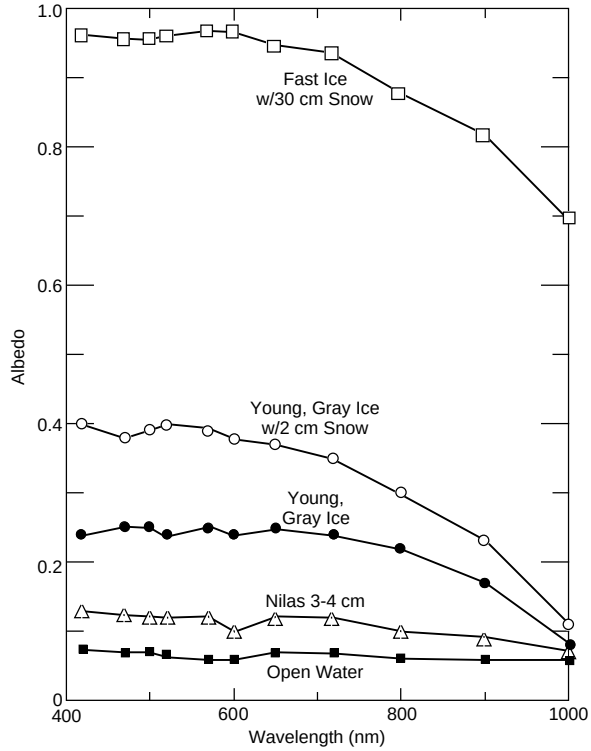

Figure 12. Spectral albedos of Antarctic sea ice (from Allison et al. 1993).

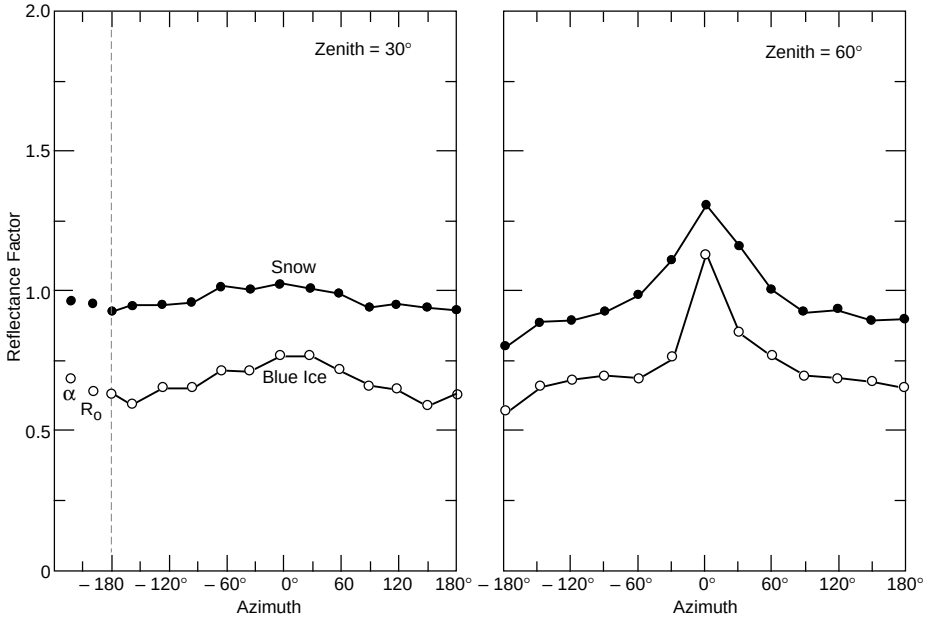

Figure 13. Bidirectional reflectance distribution function at 450 nm for snow-covered ice and bare blue ice (from Perovich 1994). R_0 is the normalized reflected radiance at nadir and α is the albedo. The measurements were made at a solar zenith angle of 60° under clear skies.

The peak in reflectance is largely due to specular reflection of the direct solar beam. Specular reflection is light reflected from the surface of the medium in the direction of the angle of reflection. Its magnitude depends on the angle of incidence and the index of refraction according to:

$$I_r(\theta) = I_0(\theta)\frac{1}{2}\left(\frac{\sin^2(\theta-\phi^*)}{\sin^2(\theta+\phi^*)} + \frac{\tan^2(\theta-\phi^*)}{\tan^2(\theta+\phi^*)}\right)$$

where $I_0(\theta)$ = the incident direct solar beam radiance,
$I_r(\theta)$ = the reflected radiance
θ = the zenith angle of incident and reflected radiance
$\theta^* = [n \arcsin(\theta)]^{-1}$
n = the index of refraction of the medium (Born and Wolfe 1965).

As the zenith angle increases (sun gets closer to the horizon), the specular reflection increases. The specular component is larger for smooth surfaces such as blue ice or melt ponds and smaller for rough surfaces such as snow or drained white ice.

Transmission

The magnitude and spectral distribution of light transmitted through the ice cover depends on the physical composition of the ice, the thickness of the ice, and the surface conditions. As thickness increases, light transmission through the ice drops off roughly exponentially. The influence of surface conditions on light transmission through the ice is illustrated in Figure 14 (Maykut and Grenfell 1975). Even a thin (0.25-m) layer of highly scattering snow can reduce transmittances through the ice cover to less than 1% (curve a). As the snow melts, scattering decreases and the transmittance increases (curve b) until the snow is gone (curve c). The presence of melt ponds greatly reduces scattering in the upper portion of the ice and enhances transmission in the visible (curve d). Light levels beneath ponded first-year ice are at least a factor of three greater than those beneath white ice of the same thickness (Grenfell and Maykut 1977).

Sea ice can be a prime habitat for biological organisms. The growth of these organisms is influenced by the amount of light available in and under the ice (Soo Hoo et al. 1987, Cota and Horne 1989, Arrigo et al. 1991). Just as the ice biota are affected by the light levels, they in turn can reduce light transmission and change its spectral composition (Maykut and Grenfell 1975, Soo Hoo et al. 1987, Perovich et al. 1993). As an example of this, spectral transmittances for 1.5-m-thick first-year ice with a 0.05-m snow cover and with a 0.19-m snow cover are plotted in Figure 15. Surprisingly, the transmission is less under the thinner snow cover. This is a direct result of a 50% higher algal biomass (157 vs. 117 mg chlorophyll m^{-2}) at the thin snow site. In addition to the overall reduction, the presence of the additional biomass results in enhanced losses in the blue end of the spectrum and a pronounced drop in transmittance at 670 nm.

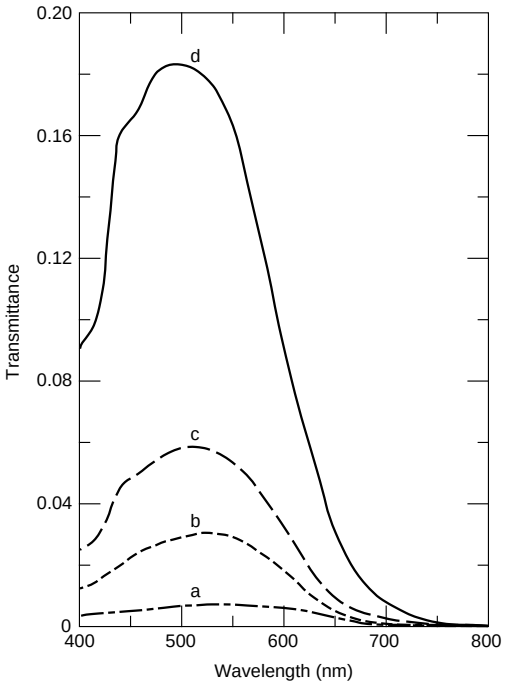

Figure 14. The influence of surface conditions on light transmission (from Maykut and Grenfell 1977). In all cases the ice thickness was 1.85 m. Surface conditions were a) blue ice covered by 0.25 m of melting snow, b) blue ice covered by 0.12 m of melting snow, c) white ice and d) blue ice covered by a 0.05-m melt pond.

Extinction coefficient

A more fundamental way to characterize light penetration through sea ice is by an extinction coefficient (κ_λ). The extinction coefficient is a measure of loss due to scattering and absorption and is typically determined from measurements of incident, reflected and transmitted light. Transmission measurements are difficult and demanding, and consequently there have been far fewer

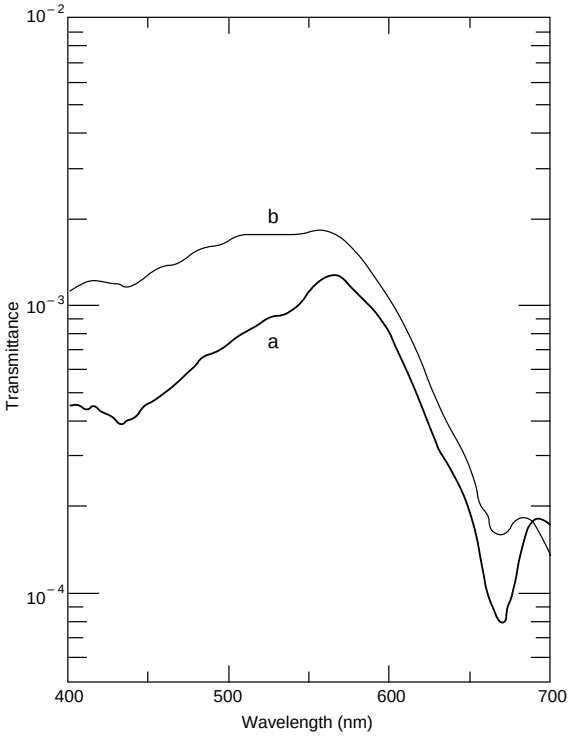

Figure 15. Observed spectral transmittances for 1.5-m-thick first-year ice with a) 0.05-m snow cover plus 157 mg chlorophyll m^{-2} biomass and b) 0.19 m snow cover plus 117 mg chlorophyll m^{-2}.

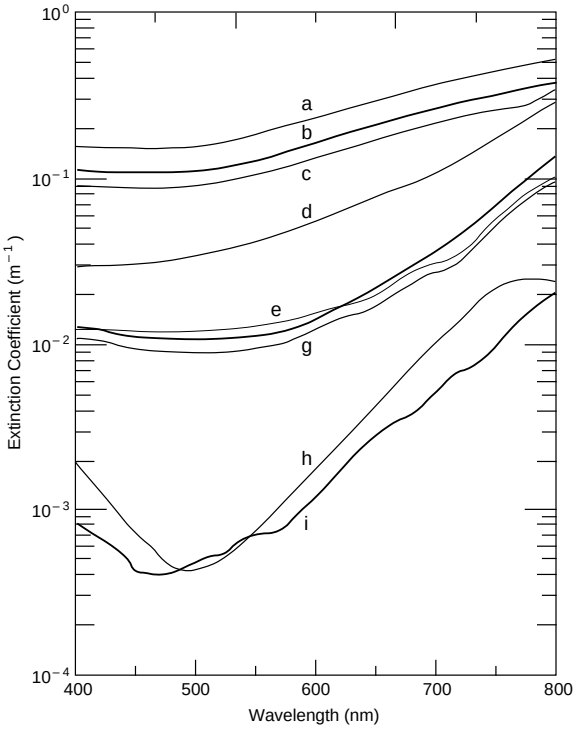

Figure 16. Spectral extinction coefficients for nine distinct cases: a) dry snow (Grenfell and Maykut 1977), b) ice below the eutectic point with solid salts present (Perovich and Grenfell 1981), c) melting snow (Grenfell and Maykut 1977), d) surface scattering layer of white ice (Grenfell and Maykut 1977), e) the interior of white ice (Grenfell and Maykut 1977), f) cold blue ice (Grenfell and Maykut 1977), g) melting blue ice (Grenfell and Maykut 1977), h) bubble-free fresh ice (Grenfell and Perovich 1981), and i) clear Arctic water (Smith and Baker 1981).

observations of extinction coefficient than of albedo. Most of the reported sea ice spectral extinction coefficients have been calculated using a two-stream radiative transfer model (Grenfell and Maykut 1977, Perovich and Grenfell 1981).

Figure 16 summarizes spectral extinction coefficients culled from a number of sources for nine distinct cases: dry snow, melting snow, ice below the eutectic point with solid salts present, the surface scattering layer of white ice, the interior of white ice, cold blue ice, melting blue ice, bubble-free fresh ice, and clear Arctic water (Grenfell and Maykut 1977, Perovich and Grenfell 1981, Smith and Baker 1981). The range of over one to two orders of magnitude in the extinction coefficients shows the tremendous variation in attenuation between different snow and ice types. Sea ice and snow curves all show relatively constant values in the 400- to 500-nm region, followed by strongly increased attenuation at longer wavelengths. Again, as was the case for albedo, the magnitude of the extinction coefficient is largely a function of the amount of scattering, while the wavelength dependence is determined by absorption. The greatest attenuation occurs in cold snow, where spectral extinction coefficients are about 20 times larger than those of melting blue ice.

Coefficients in melting snow are above half those in cold dry snow. Extinction coefficients for very cold ice below the eutectic point are quite large, comparable to values for snow. In this case solid salts precipitate in the interior of the sea ice. These precipitated salts are small and plentiful and, with an index of refraction of approximately 1.5, are effective scatterers. The drained surface layer of multiyear ice (white ice scattering) contains an abundance of air inclusions which formed as a result of brine drainage. These air inclusions cause considerable scattering, and extinction coefficients are large. In the interior of white ice there are fewer air bubbles, and extinction coefficients are correspondingly smaller. In the blue ice cases the inclusions are primarily brine pockets,

rather than air bubbles, and the amount of scattering is less and extinction coefficients are reduced. The much smaller values of extinction coefficient for bubble-free ice and clear Arctic water illustrate how significant scattering is in sea ice. The importance of scattering is illustrated by the rough rule of thumb that extinction through 1 cm of snow is approximately the same as through 10 cm of ice or 100 cm of water.

As was the case for albedo (Fig. 11), extinction coefficients also depend on the internal structure of the ice (Zaneveld 1966, Grenfell and Maykut 1977, Perovich and Grenfell 1981, Gilbert and Buntzen 1986). Extinction coefficients decrease during warming as the brine volume increases and the number of inclusions decrease. Also, at a given brine volume extinction coefficients are larger for faster grown ice, which has more inclusions. In these experiments the ice was changing internally, but the only change in surface conditions was a slight wetting as the air temperature approached 0°C. The results would be quite different if there were brine drainage from the surface layer of the ice as a result of the warming. In that case the resulting air voids would form a highly scattering surface layer, and albedos and extinction coefficients would increase. This would be expected in thicker ice with more freeboard. Such an effect has been observed in the Antarctic, where low humidities keep the ice surface free of water during melt (Andreas and Ackley 1981). Observations made in McMurdo Sound, Antarctica (Trodahl et al. 1987, Buckley and Trodahl 1987, Trodahl and Buckley 1990), have shown that as the ice warms, a drained surface layer forms resulting in an increase in backscatter and a decrease in transmittance.

Observations of total light transmission have been used to determine wavelength-integrated, or total, extinction coefficients (κ_t). Values for sea ice are in the 1.1 to 1.5 m^{-1} range (Untersteiner 1961, Chernogovskiy 1963, Thomas 1963, Weller and Schwerdtfeger 1967). Extinction coefficients for snow are much larger, varying from 4.3 m^{-1} for dense Antarctic snow (Weller and Schwerdtfeger 1967) to as high as 40 m^{-1} in freshly fallen snow (Thomas 1963). Though total extinction coefficients are simpler to measure and simpler to use computationally than spectral values, they are severely limited. The total extinction coefficient combines contributions from different wavelengths and therefore depends on the spectral distribution of transmitted irradiance, which in turn depends on the spectral incident irradiance, the spectral albedo and the spectral extinction coefficient. Since all of these quantities vary with wavelength, the total extinction coefficient does not depend entirely on the properties of the ice. As was the case for total albedo, the total extinction coefficient depends on sky conditions. On sunny days the incident irradiance has a larger longwave component, which is absorbed rapidly in the ice, resulting in higher values of κ_t. More significantly, κ_t exhibits a strong depth dependence near the surface. Observations have shown that the spectral transmittance changes greatly near the surface of the ice due to the rapid extinction of the longer wavelengths. Correspondingly, κ_t is large near the ice surface and decreases by more than an order of magnitude in the top 0.1 m of the ice (Grenfell and Maykut 1977). Below 0.1 m, only visible light remains, where the spectral dependence of κ_λ is weaker, and changes in κ_t with depth are small. Total extinction coefficients have been used in sea ice thermodynamic models (Maykut and Untersteiner 1971) to calculate the surface heat balance and solar heating in the ice interior. To do this Maykut and Untersteiner (1971) modified the exponential decay law to the form:

$$F_d(z) = i_0 F_d(0) e^{-\kappa_t z} \quad \text{for} \quad z > 0.1 \text{ m}$$

where i_0 is the fraction of the wavelength-integrated incident irradiance transmitted through the top 0.1 m of the ice and κ_t is the total extinction coefficient in the ice below 0.1 m. Values of κ_t below 0.1 m and i_0 determined from field observations (Grenfell and Maykut 1977) are summarized in Table 1. There is more scattering in white ice than blue ice, resulting in a smaller i_0 and a larger κ_t.

Table 1. Values of i_0 and κ_t (Grenfell and Maykut 1977).

Case	i_0	κ_t (m^{-1})
Clear		
Blue ice	0.43	1.5
White ice	0.18	1.6
Cloudy		
Blue ice	0.63	1.4
White ice	0.35	1.5

Beam spread

While much of the observational emphasis has been on measurements of transmitted solar irradiance to determine transmittance and extinction coefficient, measurements using artificial light

sources have also been made. In particular, studies were conducted examining the spreading of a collimated beam as it passes through sea ice (Trodahl et al. 1987, Gilbert and Schoonmaker 1990, Voss and Schoonmaker 1992, Voss et al. 1992). In these experiments a collimated beam of light was incident on either the surface or bottom of the ice and the spatial distribution of the emergent irradiance was measured. Examining the peak magnitude and the spatial distribution of irradiance provide information on scattering and absorption in the ice. Laboratory studies indicate that scattering in the ice is quite strong, with the radiation field quickly becoming diffuse, and that there is increased attenuation and scattering for colder ice (Gilbert and Schoonmaker 1990, Voss and Schoonmaker 1992). Beam spread measurements, when combined with radiative transfer models, show promise as a means of determining scattering coefficients and phase functions from multiply scattering sea ice.

MODELS

It is evident from the observational data that the optical properties of sea ice vary greatly. The optical properties vary spatially over scales of only a few meters and they vary temporally as the ice cover melts in the summer and freezes in the fall. An analysis of optical observations has demonstrated that the optical properties of sea ice are directly affected by the state and structure of the ice. Models are essential in interpreting observations and in progressing from a phenomenological collection of observations to a physically based understanding of radiative transfer in sea ice.

The variability in optical properties also creates difficulties in extrapolating observations. Individual observations provide information on the optical properties at a particular location at a particular time, but for many problems more general information is needed on how the optical properties of a region evolve with time. In principle, this information can be obtained observationally, but for a large-scale, long-term study this is not practical. For such studies, models are an essential tool.

Radiative transfer models have been applied to a wide range of problems, including estimating the absorption of solar radiation in sea ice (Maykut and Untersteiner 1971), studying the relationship between changes in ice physical properties and changes in optical properties (Grenfell 1983, 1991), analyzing the spread of a beam of light as it passes through ice (Trodahl et al. 1987), investigating bio-optical interactions (Arrigo et al. 1991), examining the transmission of visible and ultraviolet light through sea ice (Perovich 1990, 1991, 1993) and assessing radiative interactions between the atmosphere, ice and ocean (Jin et al. 1994).

These radiative transfer models for sea ice range in complexity from a simple wavelength-integrated parameterization of an exponential decay law to numerically intricate solutions of the radiance field in the ice. There are several different models with a variety of solution schemes and different input and output parameters; however, the same physics underlies all of these models. They may use different techniques but they all treat the basic physical properties of absorption and scattering of light in the ice. Because of their diversity, these models all have attributes that endorse them for some applications and restrict them for others. A sampling of sea ice radiative transfer models is presented in Table 2.

One of the distinguishing features of radiative transfer models is the number of "streams" they consider. The number of streams refers to the number of moments from which the radiance is calculated. Quite common are two-stream models, where the upwelling and downwelling irradiances are computed. More streams means more angular detail in the calculated radiance field. The cost of this additional detail is more complexity in the computations and often a requirement for more detailed information on the optical properties of the ice.

The simplest sea ice radiative transfer model is the exponential decay relationship

$$F(z,\lambda) = (1-\alpha_\lambda) F_0(\lambda) e^{-\kappa_\lambda z} \tag{5}$$

where $F_0(\lambda)$ is the incident solar irradiance. This formulation has the advantage of being simple computationally. However, there is an implicit assumption that the medium is infinitely thick, and consequently, the exponential decay law does a poor job of representing radiative transfer in thin ice (Grenfell 1979).

Grenfell (1979) developed a two-stream, three-layer model, based on the work of Dunkle and Bevans (1957), that improved the treatment of thin ice with only a modest increase in computational complexity. The general solution for the

Table 2. Summary of sea ice radiative transfer models.

Model	*Streams*	*Spectral range (nm)*	*Number of layers*	*Solution scheme*	*Output parameters*	*Comments*
Grenfell (1979)	2	400–2150	3	Analytic	F_d, F_u, α, T	Examined thin ice, developed parameterizations for α and T as a function of thickness, isotropic scattering
Perovich and Grenfell (1982)	14	400–1000	2	DOM*-analytic	$I(\theta)$, F_d, F_u, α, T	Anistropic scattering, estimate scattering parameters from observations of α and T
Grenfell (1983)	16	350–2750	1	DOM-numerical	$I(\theta)$, F_d, F_u, α, T	Detailed angular resolution, optical and physical properties are related
Trodahl et al. (1987)		500, 700	multiple	Monte Carlo	$I(\theta,x)$	Isotropic and anisotropic scattering, treats beam spread
Perovich (1990, 1993)	2	250–1000	multiple	Analytic	F_d, F_u, α, T	Ultraviolet and visible wavelengths, computationally simple, easy ice characterization, isotropic scattering
Arrigo et al. (1991)	1	400–700	multiple	Exponential	F_d, T	Detailed treatment of impact of biogenic material on light transmission
Grenfell (1992)	4	350–2750	multiple	DOM-analytic	$I(\theta)$, F_d, F_u, α, T	Tied closely to ice physical properties, treats vertical variability in ice
Jin et al. (1994)	select	250–4000	multiple	DOM-numerical	$I(\theta)$, F_d, F_u, α, T	Coupled atmosphere–ice–ocean radiative transfer absorption model, determines solar absorption in each component

*Discrete ordinates method (Chandrasekhar 1960)

upwelling (F_u) and downwelling (F_d) irradiances are

$$F_d(z,\lambda) = A\sinh(\kappa_\lambda z) + B\cosh(\kappa_\lambda z)$$

$$F_u(z,\lambda) = C\sinh(\kappa_\lambda z) + B\cosh(\kappa_\lambda z)$$

where A, B, C and D are determined from the boundary conditions. For an optically thick medium ($z \to \infty$), this solution converges to the exponential decay law (eq 5). The major deficiency of the two-stream model is its treatment of scattering, in particular, the simplifying assumption of isotropic scattering. An important advantage of this formulation is that it directly utilizes the observations of light extinction in sea ice made by Grenfell and Maykut (1977) and Perovich and Grenfell (1981). Because of this, only a qualitative description of the ice is needed; blue or white, melting or cold, snow-covered or bare. Grenfell (1979) used this model to investigate the dependence of albedo, transmittance, and i_0 on thickness and ice type. He then used the results to derive simple parameterized formulae for α_t and i_0 suitable for use in sea ice thermodynamic models.

This two-stream formulation was expanded into an n-layer model (Perovich 1990) and extended into the ultraviolet (Perovich 1993). The focus of these studies was on the spatial and temporal variability of reflection, absorption, and transmission of solar radiation by sea ice. To illustrate the utility of such models let us examine a particular problem of interest: the transmission of visible and ultraviolet light through sea ice in the Weddell Sea during spring. Spring is the period when ozone depletion is the greatest, as is the consequent increase in incident ultraviolet irradiance and potential biological hazard. Physi-

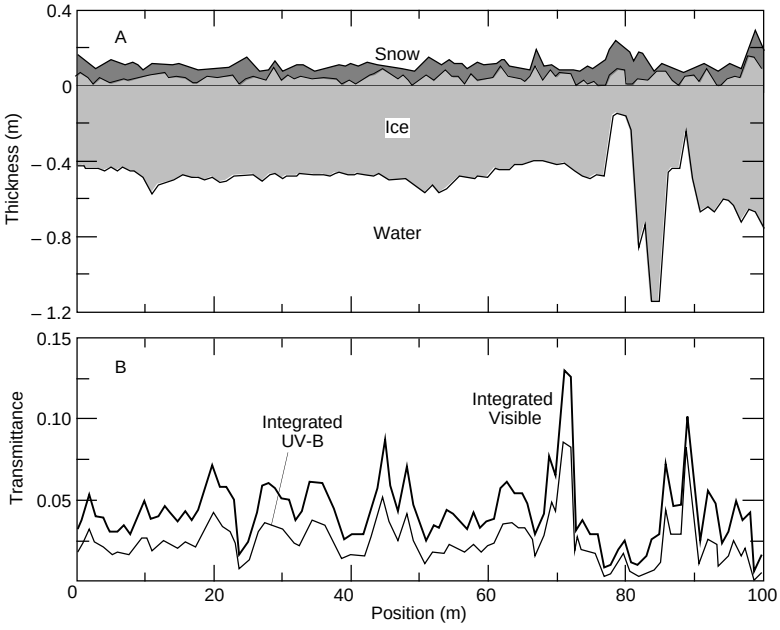

Figure 17. Theoretical estimates of ultraviolet and visible light transmission through sea ice in the Weddell Sea. Ice thickness, snow depth and physical properties data are from Lange and Eicken (1991). Transmitted UV-B and visible irradiance were computed using a two-stream model (Perovich 1990, 1993)

cal properties data from Lange and Eicken (1991) were used to define the type and thickness of the ice and snow cover (Fig. 17a) along a 100-m transect in the Weddell Sea. Ice thicknesses in this area varied from 0.2 to 1.2 m, while the snow depth ranged from 0.0 to 0.2 m. With these input parameters, the model calculated estimates of transmittance for the biologically harmful UV-B irradiance (280 to 320 nm) and the beneficial photosynthetically active radiation (400 to 700 nm) (Fig. 17b). There is tremendous spatial variability in the UV-B transmittance over the 100-m transect, with values ranging over nearly two orders of magnitude from 0.0015 to 0.09. The primary influence on transmittance is the snow depth, followed by the ice thickness. Maximum transmittances are associated with minimum snow depths. It is evident that the presence of an ice cover causes a marked reduction in transmitted light levels. This reduction is greater for the harmful UV-B than for the beneficial visible, implying that sea ice may moderate the biological impact of enhanced incident ultraviolet irradiance on biota living in and under the ice.

Models based on the discrete ordinates method (DOM) of Chandrasekhar (1960) have been used to treat scattering in more detail and examine the angular distribution of radiance. In the DOM, the phase function is approximated by a series of Legendre polynomials (Liou 1973, 1974, Mobley 1994). The discrete ordinates refer to particular angles at which the radiance is computed. These angles are not arbitrary, but are determined from the roots of the Legendre polynomial. In this formulation, it is no longer necessary to assume that the radiance field is diffuse and that the phase function is isotropic. However, these models, particularly for larger numbers of streams, are significantly more complex computationally.

Perovich and Grenfell (1982) developed a two-layer, four-stream model (radiances at two upward and two downward angles) and applied it to investigate the effects of ice thickness, and the influence of direct vs. diffuse incident solar radiation, on spectral albedo and transmittance. Using experimentally determined phase functions they found that single scattering albedos (ϖ_0) for young ice were high: from 0.95 for warm melting young ice to 0.9997 for young ice below the eutectic point.

Grenfell (1983, 1991) developed a single-layer, 16-stream model and a multilayer, four-stream model to explore relationships between ice physical properties and ice optical properties. The four-stream (Grenfell 1991) model significantly extended the work of Perovich and Grenfell (1982) by including vertically varying ice properties. The single-layer, 16-stream model (Grenfell 1983) generated a more detailed angular description of radiance, better represented the phase function, and improved the treatment of refraction at the air-ice interface for a homogeneous ice cover. This model was used to directly link the physical properties of the ice, such as the inclusion size distributions of air bubbles and brine pockets, to radiative transfer in the ice. The absorption and scattering coef-

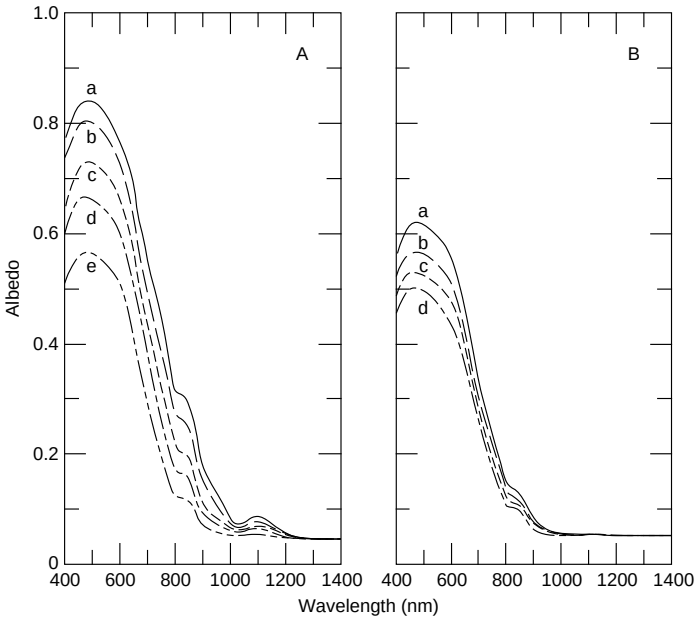

Figure 18. Calculated estimates of spectral albedo as a function of ice density and growth rate (from Grenfell 1983). The ice was 3 m thick. The air volume was zero for the growth rate simulation. Figure 18a shows albedo as a function of ice density (ρ): a) ρ = 0.86 g cm^{-3}, b) ρ=0.88 g cm^{-3}, c) ρ = 0.90 g cm^{-3}, d) ρ = 0.91 g cm^{-3} and e) ρ = 0.94 g cm^{-3}. Figure 18 shows albedo as a function of growth rate (f) for a) f = 8 × 10^{-5} cm s^{-1}, b) f = 4 × 10^{-5} cm s^{-1}, c) f = 2 × 10^{-5} cm s^{-1} and d) f = 8 × 10^{-6} cm s^{-1} .

ficients depended explicitly on the amount and size distribution of air bubbles and brine pockets. These values in turn depended on the ice growth conditions, thermal history, temperature, salinity and density. With this formulation, it was possible to theoretically explore the impact of growth conditions and thermal history on spectral albedos and extinction coefficients. For example, Figure 18 shows calculated estimates of spectral albedo for different ice densities and ice growth rates. The ice was 3 m thick in these cases. The large impact of air bubbles on scattering and ice optical properties is demonstrated in Figure 18a. There is an increase in albedo as the ice density decreases and the number of air bubbles increases. This increase is most pronounced at 470 nm, where absorption is smallest. The albedo at 470 nm was about 0.57 for bubble-free ice (ρ = 0.94) and increased to 0.84 for bubbly ice with an air volume of 8% (ρ = 0.86). Calculations also indicated that faster growth rates result in larger albedos (Fig. 18b). For these calculations the air volume was assumed to be zero, so changes in albedo resulted from changes in the platelet spacing and the number of brine inclusions. Faster grown ice has smaller platelets, higher salinity, and more brine inclusions (Weeks and Ackley 1982). This is consistent with our premise that more inclusions means more scattering and higher albedos.

The Monte Carlo method is another approach to radiative transfer modeling. As the name implies, Monte Carlo models take a statistical approach to solving the equation of radiative transfer (eq 2). In short, the absorption coefficient, the scattering coefficient and the phase function are transformed into the probability that over a given distance a photon is absorbed or scattered, and if scattered, in what direction. With these probabilities known, enormous numbers of photons are numerically "shot" into the medium. The fate of each photon is decided by the roll of the dice, or more precisely, the whim of the random number generator. Radiative transfer in the medium is described by the cumulative result of all the photons. Because of the large number of photons needed, Monte Carlo models are very inefficient computationally. They are, however, simple conceptually, simple to program, and widely applicable (Mobley 1994). This method is particularly well suited for complex geometries or boundary conditions, where other solutions to the equation of radiative transfer are difficult or impossible. Trodahl et al. (1987) and Trodahl and Buckley (1989) effectively used Monte Carlo solutions in beam spread studies, both to model observations and infer information on the scattering properties of sea ice. They found that scattering in the surface layer of the ice was greater than in the interior and that the scattering was anisotropic.

An exciting new modeling development has been the inclusion of biological effects in sea ice optical models. Sea ice is the habitat of a rich microbial community (Palmisano and Sullivan 1983, Garrison et al. 1986). Ice biota both affect and are affected by the spectral irradiance within the ice. Arrigo et al. (1991) developed a bio-optical model to investigate the interdependence between biology and transmitted light. They used a simple exponential decay law to model irradiance within the ice, but they coupled this with a sophisticated treatment of the extinction coefficients (κ). They formulated polynomial relationships defining spectral extinction coefficients for dry snow, wet snow, congelation ice, platelet ice,

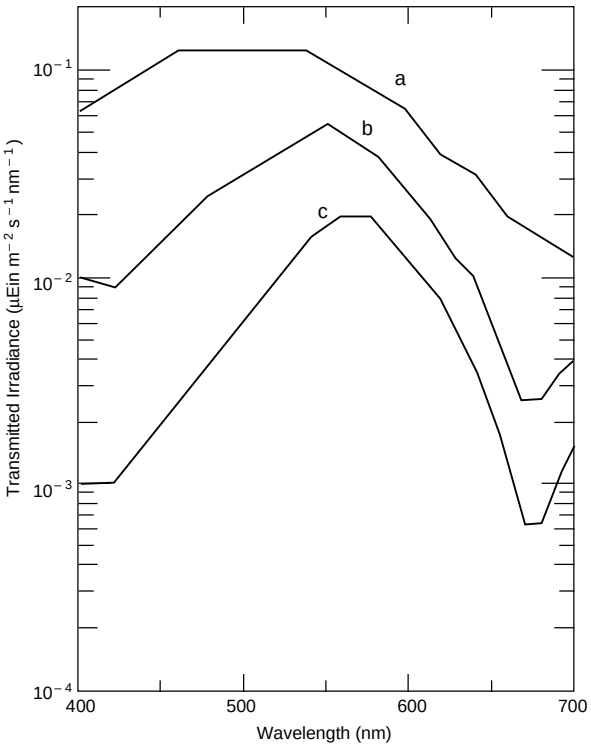

Figure 19. Seasonal changes in underice spectral irradiance calculated using a bio-optical model (Arrigo et al. 1991). Curves are predicted spectral transmitted irradiance at noon on a) 7 October 1984, b) 13 November 1984 and c) 5 December 1984.

ice cooler than the eutectic point, and as a function of brine volume. Most importantly, they also derived relationships for the extinction contributions from absorption due to microalgae and detritus. With this model it is possible to examine the impact of biogenic material on transmitted spectral irradiance and to investigate temporal changes.

Combining field observations with model calculations, Arrigo et al. (1991) were able to compute a time series of transmitted spectral irradiances (Fig. 19). The calculations were done for bare ice in McMurdo Sound, Antarctica, roughly 1.7–1.8 m thick, between 7 October and 5 December. During this period there was a constant increase in the amount of microalgae and detritus. On 7 October, levels of microalgae were low and there was no detritus present, so light losses were primarily due to extinction by the sea ice. By 13 November the spring bloom had produced significant amounts of algae and detritus. The presence of this biogenic material resulted in an overall reduction, and a change in the spectral shape, of the transmitted irradiance. The distinct spectral shape of the transmitted irradiance is characteristic of ice with biogenic material. Algae and detritus levels continued to increase through 5 December, causing a further reduction in transmittance.

A model was recently developed to examine radiative transfer in a coupled atmosphere–ice–ocean system (Jin et al. 1994). The model is a multilayer and multistream formulation based on the discrete ordinates method. Radiative transfer within the entire atmosphere–ice–ocean system is determined based on a description of physical properties of the atmosphere, ice and ocean from which the optical properties are derived. The model computes the distribution and absorption of solar radiation in the atmosphere, ice and ocean. Results indicate that sea ice has a strong influence on the distribution of solar radiation in the system (Jin et al. 1994). Such models provide a promising tool for investigating atmosphere–ice–ocean radiative feedbacks.

SUMMARY AND CURRENT AREAS OF INTEREST

By now the reader is no doubt aware that the optical properties of sea ice are variable and complex. The reader is also aware that much of this complexity is comprehensible. While many of the details still need to be determined, we do have a qualitative understanding of sea ice optical properties and their variability. This understanding is based on a few fundamental principles. Changes in such optical properties as the albedo, reflectance, transmittance, and extinction coefficient are directly tied to changes in the state and structure of the ice. Physical changes in the ice which enhance scattering, such as the formation of air bubbles due to brine drainage, result in larger albedos and extinction coefficients. Radiative transfer in sea ice is a combination of absorption and scattering. Differences in the magnitude of these optical properties are due primarily to differences in scattering. Spectral variations are mainly a result of absorption.

In addition to these general principles, there are also several specific comments that can be made regarding the sea ice optical properties. Spectral absorption coefficients for ice are well known, however, representative values for brine are less certain. Absorption by algae and particulates is also important and needs further investigation. More work, both experimental and theo-

retical, needs to be done investigating scattering in sea ice. The albedo is quite sensitive to the surface state. If the ice has an appreciable snow cover, visible wavelength albedos are above 90% and little light is transmitted to the ocean. In very cold ice (T<–24°C), hydrohalite precipitates, causing a sharp increase in albedo and extinction coefficient to values comparable to snow. There is a less pronounced, but still potentially significant, effect at temperatures below –8°C where mirabilite precipitates. The presence of liquid water on the surface causes a decrease in albedo, which is more pronounced at longer wavelengths. If the surface drains, the brine pockets become air bubbles, resulting in more scattering and an increase in albedo and extinction coefficient. Ice that is grown faster has more platelets and more brine inclusions, and consequently, large albedos and extinction coefficients. The optical properties depend not only on the volume of brine or air, but on how that brine or air is distributed.

Sea ice optical properties is currently a research area of considerable interest and activity. Even though much has been learned about the optical properties of sea ice, there are still numerous important and intriguing problems extant. A major goal is quantifying relationships between the physical and the optical properties. Achieving this goal entails not only a better understanding of the optical properties, but a better understanding of the physical properties. Because of the potential climatological impact of ice–albedo feedback, one area of particular concern is determining how the changes in the physical state of the ice during the summer melt season affect the albedo of the ice cover.

An improved understanding of scattering in sea ice is needed. This can be addressed through laboratory studies of the scattering properties of small sea ice samples (Miller et al. 1994) and through field studies investigating the spread of a collimated beam of light in ice (Longacre and Landry 1994). Another approach to estimating the scattering properties of sea ice is to use Mie theory (Bohren and Huffman 1983). A statistical description of the ice microstructure is needed for this approach, including detailed information on the inclusion size distributions for the air bubbles and brine pockets (Perovich and Gow 1991). Little is known regarding these size distributions and how they vary with ice physical properties such as brine volume, density and growth rate.

In the past there has been an abundance of albedo measurements, but few observations of transmitted light. This deficiency has impeded radiative transfer modeling efforts, ice heat balance studies, and bio-optical investigations. This is beginning to change as advancing technology leads to improved instrumentation and innovative new approaches to measuring light in and under the ice are developed. New sensors make it possible to measure detailed spectral transmittances even under thick snow-covered ice. Fiber optic probes can be frozen in the ice to measure the radiance distribution within the ice. Powerful techniques are being applied to measure in-situ profiles of transmitted irradiance, beam spread, and diffuse attenuation coefficient.*

Many pressing issues concerning sea ice optical properties can only be addressed through interdisciplinary studies. A combined effort is needed to examine such issues as assessing ice–albedo feedback, ascertaining the impact of enhanced incident levels of ultraviolet irradiance on biota living in or under the ice, and using satellite-measured microwave signatures as a proxy for large-scale ice albedo. Recent experimental programs have recognized this and have emphasized acquiring a comprehensive data set, including information on the ice state and structure, biota, particulates and microwave signatures, as well as complete optical measurements.

Another approach to these problems is through modeling, in particular through the integration of models. As the previous section demonstrated, there are several good radiative transfer models for sea ice that include information on the physical properties of the ice (Grenfell 1983, 1991, Jin et al. 1994). There are also models that treat the physical properties of sea ice during the first year of growth (Cox and Weeks 1988, Wade and Weeks in press). Thermodynamic sea ice models include, typically in a parameterized fashion, the reflection, absorption and transmission of solar radiation. The effects of biogenic material on transmitted irradiance can be considered (Arrigo et al. 1991), and there has been progress towards developing a true bio-optical model where the intricate interplay between the light levels in and under the ice and the amount of biological activity can be fully explored (Arrigo et al. 1993).

General, comprehensive, interdisciplinary models are needed models that couple the ice

* Personal communication with S. Pegau, College of Oceanic and Atmospheric Sciences, Oregon State University.

physical properties, optical properties, biological properties and thermodynamics, and that link the ice to the atmosphere and ocean. Models where changes in ice temperature cause changes in the physical properties of the ice, which in turn impact the ice optical properties and thereby the physical properties and the biological activity within the ice. Models where changes in the ice are coupled to energy exchange with the atmosphere and ocean. Developing such models is a daunting task, but a task with substantial rewards.

LITERATURE CITED

Allison, I., R.E. Brandt and S.G. Warren (1993) East Antarctic sea ice: Albedo, thickness distribution and snow cover. *Journal of Geophysical Research,* **98**(C7): 12417–12429.

Andreas, E.L. and S.F. Ackley (1981) On the differences in ablation seasons of the Arctic and Antarctic sea ice. *Journal of Atmospheric Science*, **39**: 440–447.

Arrigo, K.R., J.N. Kremer, and C.W. Sullivan (1993) A simulated Antarctic fast ice ecosystem. *Journal of Geophysical Research,* **98**(C4): 6929–6946.

Arrigo, K.R., C.W. Sullivan and J. N. Kremer (1991) A bio-optical model of Antarctic sea ice. *Journal of Geophysical Research,* **96**: 10581–10592.

Bohren, C.F. and B.R. Barkstrom (1974) Theory of the optical properties of snow. *Journal of Geophysical Research,* **79**(30): 4527–4535.

Bohren, C.F. and D.R. Huffman (1983) *Absorption and Scattering of Light by Small Particles*. New York: Wiley.

Born, M. and E. Wolfe (1965) *Principles of Optics*. New York: Pergamon.

Buckley, R.G. and H.J. Trodahl (1987) Thermally driven changes in the optical properties of sea ice. *Cold Regions Science and Technology,* **14**: 201–204.

Burt, W.V. (1954) Albedo over wind roughened water. *Journal of Meteorology,* **11**: 283–290.

Chandrasekhar, S.C. (1960) *Radiative Transfer*. New York: Dover.

Chernigovskiy, N.T. (1963) Radiational properties of the central Arctic ice cover. *Trudy Arkticheskogo I Antarkticheskogo Nauchno-Issledovatel'skogo Instituta,* Tom **253**: 249–260.

Cota, G.F. and E.P.W. Horne (1989) Physical control of Arctic ice algal production. *Mar. Ecol. Prog. Ser.,* **52**: 111–121.

Cox, G.F.N. and W.F. Weeks (1988) Numerical simulations of the profile properties of undeformed first-year sea ice during the growth season. *Journal of Geophysical Research,* **93**: 12,449–12461.

Dunkle, R.V. and J.T. Bevans (1957) An approximate analysis of the solar reflectance and transmittance of a snow cover. *Journal of Meteorology,* **13**: 212–216.

Ebert, E.E. and J.A. Curry (1993) An intermediate one-dimensional thermodynamic sea ice model for investigating ice-atmosphere interactions. *Journal of Geophysical Research,* **98**: 10085–10019.

Frederick, J.E. and D. Lubin (1988) The budget of biologically active ultraviolet radiation in the earth-atmosphere system. *Journal of Geophysical Research,* **93**: 3825–3832.

Garrison, D.L., C.W. Sullivan and S.F. Ackley (1986) Sea ice microbial communities in Antarctica. *BioScience*, **36**: 243–250.

Gilbert, G.D. and R.R. Buntzen (1986) In-situ measurements of the optical properties of Arctic sea ice. In *Proceedings of SPIE Ocean Optics VIII*, **637**: 252–263.

Gilbert, G.D. and J. Schoonmaker (1990) Measurements of beam spread in new ice. In *Proceedings of SPIE Ocean Optics VIII*, **1302**: 545–555.

Gow, A.J. and W.B. Tucker, III (1990) Sea ice in the polar regions. In *Polar Oceanography, Part A: Physical Science* (Walker O. Smith, Ed.), p. 47–122. San Diego: Academic Press.

Grenfell, T.C. (1979) The effects of ice thickness on the exchange of solar radiation over the polar oceans. *Journal of Glaciology,* **22**: 305–320.

Grenfell, T.C. (1983) A theoretical model of the optical properties of sea ice in the visible and near infrared. *Journal of Geophysical Research,* **88**: 9723–9735.

Grenfell, T.C. (1991) Radiative transfer model for sea ice with vertical structure variations. *Journal of Geophysical Research,* **96**: 16991–17001.

Grenfell, T.C. and D. Hedrick (1983) Scattering of visible and near infrared radiation by NaCl ice and glacier ice. *Cold Regions Science and Technology,* **8**: 119–127.

Grenfell, T.C. and G.A. Maykut (1977) The optical properties of ice and snow in the Arctic Basin. *Journal of Glaciology,* **18***:* 445–463.

Grenfell, T.C. and D.K. Perovich (1981) Radiation absorption coefficients of polycrystalline ice from 400–1400 nm. *Journal of Geophysical Research,* **86**: 7447–7450.

Grenfell, T.C. and D.K. Perovich (1984) Spectral albedos of sea ice and incident solar irradiance in the southern Beaufort Sea. *Journal of Geophysical Research,* **89**: 3573–3580.

Ingram, W.J., C.A. Wilson and J.F.B. Mitchell (1989) Modeling climate changes: An assessment of sea ice and surface albedo feedbacks. *Journal of Geophysical Research,* **94**(D6): 8609–8622.

Jin, Z., K. Stamnes, and W.F. Weeks (1994) The effect of sea ice on the solar energy budget in the atmosphere-sea ice-ocean system: A model study. *Journal of Geophysical Research,* **99**(C12), 25281–25294.

Lange, M.A. and H. Eicken (1991) The sea ice thickness distribution in the northwestern Weddell Sea. *Journal of Geophysical Research,* **96**: 4821–4837.

Langleben, M.P. (1971) Albedo of melting sea ice in the southern Beaufort Sea. *Journal of Glaciology,* **10**: 101–104.

Light, B. (1995) A structural-optical model of cold sea ice. M.S. Thesis, University of Washington, Seattle (unpublished).

Liou, K.N. (1973) A numerical experiment on Chandrasekhar's discrete ordinates method for radiative transfer: Applications to cloudy and hazy atmospheres. *Journal of Atmospheric Sciences,* **30**: 1303–1326.

Liou, K.N. (1974) Analytic two-stream and four-stream solutions for radiative transfer. *Journal of Atmospheric Sciences,* **31**: 1473–1475.

Lofgren, G. and W.F. Weeks (1969) Effects of growth parameters on substructure spacing in NaCl ice crystals. *Journal of Glaciology,* **8**: 153–164.

Longacre, J.R. and M.A. Landry (1994) In-situ measurements of optical scattering from the water-ice interface of sea ice. In *Proceedings of SPIE Ocean Optics XII,* **2258**: 944–954.

Lubin, D., J.E. Frederick and A.J. Krueger (1989) The ultraviolet radiation environment of Antarctica: McMurdo Station during September–October 1987. *Journal of Geophysical Research,* **94**: 8491–8496.

Maykut, G.A. (1982) Large-scale heat exchange and ice production in the central Arctic. *Journal of Geophysical Research,* **87**: 7971–7985.

Maykut, G. A. and T. C. Grenfell (1975) The spectral distribution of light beneath first-year sea ice in the Arctic Ocean. *Limnology and Oceanography*, **20**: 554–563.

Maykut, G.A. and B. Light (1995) Refractive index measurements in freezing sea ice and sodium chloride brines. *Applied Optics*, **34**: 950–961.

Maykut, G.A. and D.K. Perovich (1987) On the role of shortwave radiation in the summer decay of a sea ice cover. *Journal of Geophysical Research,* **92**(C7): 7032–7044.

Maykut, G.A. and N. Untersteiner (1971) Some results from a time dependent, thermodynamic model of sea ice. *Journal of Geophysical Research,* **76**: 1550–1575.

Miller, D. M.S. Quinby-Hunt and A.J. Hunt (1994) Polarization-dependent measurements of light scattering in sea ice. *Proceedings of SPIE Ocean Optics XII,* **2258**: 908–920.

Mobley, C.D. (1994) *Light and Water: Radiative Transfer in Natural Waters*. San Diego: Academic Press.

Nicodemus, F.E., J.C. Richmond, J.J. Hsia, I.W. Ginsberg and T. Limperis (1977) Geometrical considerations and nomenclature for reflectance. *NBS Monograph 160*, U.S.

Palmisano, A.C. and C.W. Sullivan (1983) Sea ice microbial communities (SIMCO): I. Distribution, abundance and primary production of ice microalgae in McMurdo Sound, Antarctica in 1980. *Polar Biology,* **2**: 171.

Perovich, D.K. (1979) *The Optical Properties of Young Sea Ice.* M.S. Thesis (unpublished), Geophysics Program, University of Washington, Seattle, Washington (Office of Naval Research Contract N00014-76-C-0234, Scientific Report No. l7, Department of Atmospheric Sciences, University of Washington, Seattle).

Perovich, D.K. (1990) Theoretical estimates of light reflection and transmission by spatially complex and temporally varying sea ice covers. *Journal of Geophysics,* **95**: 9557–9567.

Perovich, D.K. (1991) Seasonal changes in sea ice optical properties during fall freeze-up. *Cold Regions Science and Technology,* **19**: 261–273.

Perovich, D.K. (1993) A theoretical model of ultraviolet light transmission through Antarctic sea ice. *Journal of Geophysical Research,* **98**: 22,579–22,587.

Perovich, D.K. (1994) Light reflection from sea ice during the onset of melt. *Journal of Geophysical Research,* **99**: 3351–3359.

Perovich, D.K. and J.W. Govoni (1991) Absorption coefficients of ice from 250 to 400 nm. *Geophysical Research Letters,* **18**: 1233–1235.

Perovich, D.K. and A.J. Gow (1991) A statistical description of the microstructure of young sea ice. *Journal of Geophysical Research,* **96**: 16,943–16,953.

Perovich, D.K. and T.C. Grenfell (1981) Laboratory studies of the optical properties of young sea ice. *Journal of Glaciology*, **27**: 331–346.

Perovich, D.K. and T.C. Grenfell (1982) A theoretical model of radiative transfer in young sea ice. *Journal of Glaciology*, **28**: 34l–357.

Perovich, D.K. and G.A. Maykut (1990) The treatment of shortwave radiation and open water in

large-scale models of sea ice decay. *Annals of Glaciology,* **14**: 242–246.

Perovich, D.K., G.A. Maykut and T.C. Grenfell (1986) Optical properties of ice and snow in the polar oceans: I. Observations. *Proceedings of SPIE Ocean Optics VIII,* **637**: 232–241.

Perovich, D.K., G.F. Cota, G.A. Maykut and T.C. Grenfell (1993) Bio-optical observations of first-year Arctic sea ice. *Geophysical Research Letters,* **20**: 1059–1062.

Roesler, C. and R. Iturriaga (1994) Absorption properties of marine-derived material in Arctic sea ice. *Proceedings of SPIE Ocean Optics XII,* **2258**: 933–944.

Schlosser, E. (1988) Optical studies of Antarctic sea ice. *Cold Regions Science and Technology,* **15**: 289-293.

Smith, R.C. (1989) Ozone, middle ultraviolet radiation and the aquatic environment. *Photochemistry and Photobiology,* **50**: 459–468.

Smith, R.C. and K.S. Baker (1981) Optical properties of the clearest natural waters (200–800 nm). *Applied Optics,* **20**: 177–184.

Smith, R.C., W. Zhengming and K.S. Baker (1992a) Ozone depletion in Antarctica: Modeling its effect on solar UV irradiance under clear-sky conditions. *Journal of Geophysical Research,* **97**: 7383–7397.

Smith, R.C., B.B. Prezelin, K.S. Baker, R.R. Bidigare, N.P. Boucher, T. Coley, D. Karentz, S. MacIntyre, H.A. Matlick, D. Menzies, M. Ondrusek, Z. Wan and K.J. Waters (1992b) Ozone depletion: Ultraviolet radiation and phytoplankton biology in Antarctic waters. *Science*, **255**: 952–959.

SooHoo, T.B., A.C. Palmisano, S.T. Kottmeier, M.P. Lizotte, S.L. SooHoo and C.W. Sullivan (1987) Spectral light absorption and quantum yield of photosynthesis in sea ice microalgae and a bloom of *Phaeocystis pouchettii* from McMurdo Sound, Antarctica. *Marine Ecology*, **33**: 175–189.

Thomas, C.W. (1963) On the transfer of visible radiation through sea ice and snow. *Journal of Glaciology,* **4**: 481–484.

Thorndike, A.S. (1992) A toy model linking atmospheric thermal radiation and sea ice growth. *Journal of Geophysical Research,* **97**(C6): 9401–9410.

Trodahl, H.J. and R.G. Buckley (1989) Ultraviolet levels under sea ice during the Antarctic spring. *Science,* **245**: 194–195.

Trodahl, H.J. and R.G. Buckley (1990) Enhanced ultraviolet transmission of Antarctic sea ice during the austral spring. *Geophysical Research Letters,* **17**: 2177–2179

Trodahl, H.J., R.J. Buckley and S. Brown (1987) Diffusive transport of light in sea ice. *Applied Optics*, **26**: 3005–3011.

Tsay, S. and K. Stamnes (1992) Ultraviolet radiation in the Arctic: The impact of potential ozone depletions and cloud effects. *Journal of Geophysical Research,* **97**: 7829–7840.

Tyler, J.E., and R.C. Smith (1970) *Measurements of Spectral Radiance Underwater.* New York: Gordon and Breach.

Untersteiner, N. (1961) On the mass and heat budget of Arctic sea ice. *Arch. Meteorol. Geophys. Bioklim., Series A,* **12**: 151–182.

van de Hulst, H.C. (1981) *Light Scattering by Small Particles*. New York: Dover.

Voss, K.J. and J.S. Schoonmaker (1992) Temperature dependence of beam scattering in young sea ice. *Applied Optics*, **31**: 3388–3389.

Voss, K.J. R.C. Honey, G.D. Gilbert and R.R. Buntzen (1992) Measuring the point spread function of sea ice *in situ*. In *Proceedings of SPIE Ocean Optics XI*, **1750**: 517–522.

Wade R.H. and W.F. Weeks (in press) Radar backscatter estimates from a combined ice growth and surface scattering model of first-year sea ice. *EARSel*.

Warren, S.G. (1982) Optical properties of snow. *Review of Geophysics and Space Physics,* **20**: 67–89.

Weeks, W.F. and S.F. Ackley (1982) The growth, structure, and properties of sea ice. USA Cold Regions Research and Engineering Laboratory, Monograph 82-1.

Weeks, W.F. and W.L. Hamilton (1962) Petrographic characteristics of young sea ice, Point Barrow, Alaska. *American Mineralogy,* **47**: 945–961.

Weller, G. (1972) Radiation flux investigations. *AIDJEX Bulletin,* **14**: 28–30.

Weller, G. and P. Schwerdtfeger (1967) Radiation penetration in antarctic plateau and sea ice. In *Polar Meteorology, World Meteorological Organization Technical Note No. 87*, p. 120–141.

Wiscombe, W.J. and S.G. Warren (1980) A model for the spectral albedo of snow, 1, Pure snow. *Journal of Atmospheric Science,* **37**(12): 2712–2733.

Zaneveld, J.R.V. (1964) The transparency of sea ice in the visible region. M.S. Thesis, Massachusetts Institute of Technology (unpublished).

APPENDIX A: LIST OF SYMBOLS

E_0	radiance of the direct beam component of the incident radiation field
f	growth rate
F	irradiance
F_d	downwelling irradiance
F_u	upwelling irradiance
I	radiance
i_0	fraction of incident irradiance transmitted through the top 0.1 m of the ice
I_r	reflected radiance
k_b	absorption coefficient of brine
k_i	absorption coefficient of ice
k_si	absorption coefficient of sea ice
N	real index of refraction
$p(\mu, \mu', \phi, \phi')$	phase function
R	bidirectional reflectance distribution function (BRDF)
R_0	normalized reflected radiance at nadir
S	source function
T	transmittance
x	horizontal position
z	depth within the medium
α	albedo
α_t	wavelength-integrated, or total, albedo
ϕ	azimuth angle
ϕ_0	solar azimuth angle
κ	extinction coefficient
κ_t	wavelength-integrated, or total, extinction coefficients
λ	wavelength
ν_s	volume fraction of ice
ν_b	volume fraction of brine
θ	zenith angle (0 pointing downward, π pointing upward)
θ_0	solar zenith angle
μ	cosine of the zenith angle, θ
ρ	density
σ	scattering coefficient
τ	nondimensional optical depth
ϖ_0	single scattering albedo

REPORT DOCUMENTATION PAGE

Form Approved
OMB No. 0704-0188

1. AGENCY USE ONLY (Leave blank)	2. REPORT DATE	3. REPORT TYPE AND DATES COVERED
	May 1996	

4. TITLE AND SUBTITLE

The Optical Properties of Sea Ice

5. FUNDING NUMBERS

Office of Naval Research
Contracts
N0001495MP30002
N0001495MP30031

6. AUTHORS

Donald K. Perovich

7. PERFORMING ORGANIZATION NAME(S) AND ADDRESS(ES)

U.S. Army Cold Regions Research and Engineering Laboratory
72 Lyme Road
Hanover, New Hampshire 03755-1290

8. PERFORMING ORGANIZATION REPORT NUMBER

Monograph 96-1

9. SPONSORING/MONITORING AGENCY NAME(S) AND ADDRESS(ES)

Office of Naval Research
800 N. Quincy Street
Arlington, Virginia 22217-5000

10. SPONSORING/MONITORING AGENCY REPORT NUMBER

11. SUPPLEMENTARY NOTES

12a. DISTRIBUTION/AVAILABILITY STATEMENT

Approved for public release; distribution is unlimited.

Available from NTIS, Springfield, Virginia 22161

12b. DISTRIBUTION CODE

13. ABSTRACT (*Maximum 200 words*)

Sea ice is a translucent material with an intricate structure and complex optical properties. Understanding the reflection, absorption, and transmission of shortwave radiation by sea ice is important to a diverse array of scientific problems, including those in ice thermodynamics and polar climatology. Radiative transfer in sea ice is a combination of absorption and scattering. Differences in the magnitude of sea ice optical properties are due primarily to differences in scattering. Spectral variations are mainly a result of absorption. Changes in such optical properties as the albedo, reflectance, transmittance, and extinction coefficient are directly related to changes in the state and structure of the ice. Physical changes that enhance scattering, such as the formation of air bubbles due to brine drainage, result in larger albedos and extinction coefficients. The albedo is quite sensitive to the surface state. If the ice has a snow cover, albedos are large. In contrast, the presence of liquid water on a bare ice surface causes a decrease in albedo, which is more pronounced at longer wavelengths. Sea-ice optical properties depend on the volume of brine and air and on how the brine and air are distributed.

14. SUBJECT TERMS

Albedo
Absorption
Optical properties
Scattering
Sea ice

15. NUMBER OF PAGES

33

16. PRICE CODE

17. SECURITY CLASSIFICATION OF REPORT	18. SECURITY CLASSIFICATION OF THIS PAGE	19. SECURITY CLASSIFICATION OF ABSTRACT	20. LIMITATION OF ABSTRACT
UNCLASSIFIED	UNCLASSIFIED	UNCLASSIFIED	UL